



## Molecular phylogenetics and historical biogeography of the west-palearctic common toads (*Bufo bufo* species complex)

J. Garcia-Porta<sup>a</sup>, S.N. Litvinchuk<sup>b</sup>, P.A. Crochet<sup>c</sup>, A. Romano<sup>d</sup>, P.H. Geniez<sup>c</sup>, M. Lo-Valvo<sup>e</sup>, P. Lymberakis<sup>f</sup>, S. Carranza<sup>a,\*</sup>

<sup>a</sup> Institute of Evolutionary Biology (CSIC-UPF), Passeig Marítim de la Barceloneta, 37-49, 08003 Barcelona, Spain

<sup>b</sup> Institute of Cytology, Russian Academy of Sciences, Tikhoretsky pr. 4, 194064 St. Petersburg, Russia

<sup>c</sup> CNRS – UMR 5175, Centre d'Ecologie Fonctionnelle et Evolutive, 1919 Route de Mende, F-34293 Montpellier Cedex 5, France

<sup>d</sup> Dipartimento di Biologia, Università di Roma "Tor Vergata", Via della Ricerca Scientifica, I-00133 Rome, Italy

<sup>e</sup> Dipartimento di Biologia ambientale e biodiversità, Via Archirafi 18, I-90123 Palermo, Italy

<sup>f</sup> Natural History Museum of Crete, University of Crete, Knosou Av., PO Box 2208, 71409 Irakleio, Greece

### ARTICLE INFO

#### Article history:

Received 27 May 2011

Revised 18 December 2011

Accepted 20 December 2011

Available online 30 December 2011

#### Keywords:

Amphibian

Phylogeny

Biogeography

Deserts

Diversification

Pleistocene glaciations

### ABSTRACT

In most pan-Eurasian species complexes, two phenomena have been traditionally considered key processes of their cladogenesis and biogeography. First, it is hypothesized that the origin and development of the Central Asian Deserts generated a biogeographic barrier that fragmented past continuous distributions in Eastern and Western domains. Second, Pleistocene glaciations have been proposed as the main process driving the regional diversification within each of these domains. The European common toad and its closest relatives provide an interesting opportunity to examine the relative contributions of these paleogeographic and paleoclimatic events to the phylogeny and biogeography of a widespread Eurasian group. We investigate this issue by applying a multiproxy approach combining information from molecular phylogenies, a multiple correspondence analysis of allozyme data and species distribution models. Our study includes 304 specimens from 164 populations, covering most of the distributional range of the *Bufo bufo* species complex in the Western Palearctic. The phylogenies (ML and Bayesian analyses) were based on a total of 1988 bp of mitochondrial DNA encompassing three genes (*tRNA<sup>Val</sup>*, *16S* and *ND1*). A dataset with 173 species of the family Bufonidae was assembled to estimate the separation of the two pan-Eurasian species complexes of *Bufo* and to date the main biogeographic events within the *Bufo bufo* species complex. The allozyme study included sixteen protein systems, corresponding to 21 presumptive loci. Finally, the distribution models were based on maximum entropy. Our distribution models show that Eastern and Western species complexes are greatly isolated by the Central Asian Deserts, and our dating estimates place this divergence during the Middle Miocene, a moment in which different sources of evidence document a major upturn of the aridification rate of Central Asia. This climate-driven process likely separated the Eastern and Western species. At the level of the Western Palearctic, our dating estimates place most of the deepest phylogenetic structure before the Pleistocene, indicating that Pleistocene glaciations did not have a major role in splitting the major lineages. At a shallow level, the glacial dynamics contributed unevenly to the genetic structuring of populations, with a strong influence in the European–Caucasian populations, and a more relaxed effect in the Iberian populations.

© 2011 Elsevier Inc. All rights reserved.

### 1. Introduction

Throughout the Neogene (23–2.6 Ma), the Palearctic region has experienced several climatic and physiographic changes that have modulated the diversification of its biotas and shaped their distributions. This is particularly true for pan-Eurasian groups with distributions extending from the Western to the Eastern Palearctic; several paleoclimatic or paleogeographic events ranging from a re-

gional to a global scale (Blondel and Aronson, 1999; Azanza et al., 2000; Fortelius et al., 2002; Melville et al., 2009) have likely structured these populations. Singularly, the rise of the Himalayas is one of the most important landmarks for understanding the distribution patterns in the Palearctic. This process, initiated 45–55 Ma, is considered the continents' largest perturbation to atmospheric circulation, ultimately originating the Central Asian Deserts and the monsoon-like climate in Eastern Asia (Molnar et al., 2010). Several cases of sister-species complexes at both sides of the deserts have led to the hypothesis that the origin of the Central Asian Deserts separated many Eastern and Western species complexes by

\* Corresponding author. Fax: +34 93 230 95 55.

E-mail address: [salvador.carranza@ibe.upf-csic.es](mailto:salvador.carranza@ibe.upf-csic.es) (S. Carranza).

vicariance (Savage, 1973; Borkin, 1984; Voelker, 1999). For amphibians, Savage (1973) and Borkin (1984) hypothesized that the progressive aridification of Central Asia coupled with global cooling trends during the Miocene (23–5.3 Ma) forced the amphibian faunas to retract their ranges to the South, forming isolates at both sides of the great Central Asian Deserts.

After the above-mentioned splits between Eastern and Western domains, each lineage diversified regionally throughout the rest of the Neogene. However, the major causes of these cladogenetic events in most cases are debated. In the Western Palearctic, the classic “glacial refugia” theory attempts to explain most of these cladogenetic events as a consequence of shifts in the distributional ranges towards the South during the glacial maxima, leading to subsequent allopatric isolation and genetic differentiation in the Mediterranean Peninsulas (Hewitt, 2000). The existence of species or subspecies broadly dividing into Eastern and Western groups backed this theory (e.g. *Pelobates cultripes*/*Pelobates fuscus*), suggesting that both groups were derived from refugia located in different Mediterranean Peninsulas (mainly Iberian Peninsula, Italian Peninsula and the Balkans) (Llorente et al., 1995). However, dating estimates revealed that although some of the splits were associated with the glacial cycles, this was not a general rule and many splits could be firmly placed in Pre-Pleistocene times (Seddon et al., 2001; Babik et al., 2007). Therefore, the role of Pleistocene glacial cycles shifted from being one of the most important processes for explaining the current diversity of species in the Palearctic to a more labile process with different degrees of relevance depending on the particular organism and the temporal scale considered (Klicka and Zink, 1997; Soria-Carrasco and Castresana, 2011). A more modern view is that the phylogeographic structure of most Palearctic groups is actually a combination of deep splits during the Miocene or Pliocene, followed by a re-structuring caused by fluctuations in population sizes experienced during the Quaternary (e.g. Paulo et al., 2001; Mattocchia et al., 2005; Nascetti et al., 2005; Ursenbacher et al., 2008). Nevertheless, in most cases the historical causes of these deep splits usually remain elusive.

Amphibians constitute a very good model to explore the historical aspects of species distributions due to their low dispersal capacity and retention of a strong phylogeographic signal. Moreover, they are very sensitive to climatic changes, which make them optimal organisms for discriminating the effects of glacial cycles and other environmental changes upon their genetic structure and biogeographic patterns (Zeisset and Beebe, 2008). The European common toad belongs to the genus *Bufo* (*sensu stricto*), a pan-Eurasian group comprising two species complexes. Eastern Eurasia contains the greatest species richness of the genus, with 13–14 recognized species distributed across Central and Eastern China, Northern Vietnam, Korea, far Eastern Russia, and Japan (here and after the *Bufo gargarizans* species complex) (Frost, 2011; see also Zhan and Fu, 2011).

The second complex occurs in the Western Palearctic, and only two or three valid species are currently recognized (here and after the *Bufo bufo* species complex) (Litvinchuk et al., 2008; Frost, 2011): the Eichwald toad (*Bufo eichwaldi* Litvinchuk et al., 2008), restricted to the Talysh mountains of the Southeastern Caucasus; the Caucasian toad (*Bufo verrucosissimus* (Pallas, 1814), not recognized by e.g. Crochet and Dubois, 2004), which inhabits the Caucasus and Anatolia; and the European common toad (*Bufo bufo* (Linnaeus, 1758)), the Palearctic anuran with the largest distributional range, spanning from North Africa to the Polar circle and from the Western Iberian Peninsula to the Baikal Lake in Siberia (Lizana, 2002). Despite this huge distributional range, according to Mertens and Wermuth (1960), the European common toad is a single species with three subspecies: (1) the nominate subspecies *Bufo bufo bufo*, the Eurosiberian form, distributed across Northern

and Central Europe, Western Siberia, the British Islands and the Eurosiberian enclaves of the Mediterranean peninsulas, (2) *Bufo bufo spinosus* Mertens, 1925, considered the Mediterranean counterpart of the nominal subspecies, occupying the Mediterranean margins of Europe, North Africa and most parts of Western and Central France (Geniez and Cheylan, 2005, in press), and (3) *Bufo bufo gredosicola* Müller & Hellmich, 1925, with a very limited distributional range restricted to the highest prairies and lakes of the Sierra de Gredos, in Central Iberian Peninsula.

Since the European common toad and its closest relatives present a disjunct distribution across Eurasia (Lizana, 2002), and also show regional structure in the Western Palearctic, they provide an interesting opportunity to examine the importance of the Central Asian Deserts as the vicariant event that separated Eastern and Western species complexes, and secondly to assess the relative contribution of both glacial and preglacial events in the regional structure of the Western Palearctic.

The aim of the present study is to combine data from molecular phylogenies, multiple correspondence analyses of allozyme data and species distribution models, to unravel the historical processes that have contributed to shaping the biogeography and cladogenesis of the most abundant and widely distributed amphibian genus in the Palearctic.

## 2. Methods

### 2.1. Taxon sampling, DNA extraction, amplification and sequencing

A total of 151 specimens were included in the mitochondrial DNA study, covering the entire distribution range of the species complex in the Western Palearctic (Table 1 and Fig. 1). Of these, 147 are members of the *Bufo bufo* species complex, with four specimens obtained from GenBank (Benson et al., 2008). The remaining four specimens belong to the *Bufo gargarizans* species complex and were used as outgroups (all obtained from GenBank). A list of all the samples used in the present work with their extraction codes, voucher references, corresponding localities and GenBank accession numbers can be found in Table 1. Genomic DNA was extracted from ethanol-preserved tissue samples using the Qiagen DNeasy Blood & Tissue Kit. A total of 1988 bp of mitochondrial DNA were sequenced for most of the specimens (5.8% of missing data), encompassing fragments of three genes: *tRNAval* (48 bp), *16SrRNA* (1386 bp) and *ND1* (554 bp). Already published primers for the amplification and sequencing of the mitochondrial gene fragments included in the present study as well as PCR conditions used are given in detail in Biju and Bossuyt (2003) and Roelants and Bossuyt (2005). All amplified fragments were sequenced for both strands. Contigs were assembled in Geneious v. 5.3.6 (Biomatters Ltd.).

### 2.2. Phylogenetic analyses of mitochondrial DNA

The sequences obtained were aligned using the online version of MAFFT 6.240 (Katoh et al., 2002) (<http://align.bmr.kyushu-u.ac.jp/mafft/online/server/>), following a FFT-NS-i strategy (slow, iterative refinement method) with the rest of the settings left by default (scoring matrix 200PAM ( $k=2$ ), gap opening penalty = 1.53). The gaps generated by the process of alignment were considered missing data in all the following analyses.

Two methods of phylogenetic analysis, namely maximum likelihood (ML) and Bayesian analysis (BI), were employed and their results compared. The ML analysis was performed using RaxML 7.0.4 (Stamatakis, 2006) with the dataset split in two partitions: one partition including the RNA-coding genes and the other including the protein-coding gene (*ND1*). JModeltest (Posada, 2008) was used to select the most appropriate model of sequence evolution

**Table 1**

Sampling localities for the mitochondrial phylogeny and allozyme analysis (including geographic coordinates and country), taxonomic assignation and clade or group assignation according to the molecular phylogeny or the MCA analysis, respectively. A map with the geographic distribution of all the representatives of the *Bufo bufo* species complex included in our analyses is shown in Fig. 1.

Specimen number	Data Type	Latitude	Longitude	Locality	Country	Taxon	Clade/MCA group	VOUCHER	GenBankt RNA-16S 1 <sup>st</sup> part	GenBank16S 2 <sup>nd</sup> part	GenBank ND1
1	DNA	42.42139	-3.6445	Zuriza	Spain	<i>B. b. bufo</i>	Iberian		JQ348599	JQ348742	JQ348501
2	DNA	43.1224	-3.7149	Vega de Pas 1	Spain	<i>B. b. bufo</i>	Iberian		JQ348581	JQ348724	JQ348497
3	DNA	43.1272	-3.7263	Vega de Pas 2	Spain	<i>B. b. bufo</i>	Iberian		JQ348585	JQ348728	JQ348527
4	DNA	43.3202	-5.3521	Valle del Tendí	Spain	<i>B. b. bufo</i>	Iberian		JQ348563	JQ348706	JQ348500
5	DNA	42.4514	-3.6450	Udiema river	Spain	<i>ambiguous</i>	Iberian		JQ348550	JQ348693	JQ348524
6	DNA	42.3414	1.7586	Torrent del Pi	Spain	<i>B. b. spinosus</i>	Iberian		JQ348556	JQ348699	JQ348529
7	DNA	39.7717	-6.0143	Torrejon el Rubio	Spain	<i>B. b. spinosus</i>	Iberian		FJ882841		
8	DNA	45.8162	2.3252	Tigouleix	France	<i>B. b. spinosus</i>	Iberian			JQ348687	
9	DNA	41.9215	0.7185	Tartareu	Spain	<i>B. b. spinosus</i>	Iberian		JQ348560	JQ348703	JQ348486
10	DNA	42.3686	2.9807	St. Climent Sescibes	Spain	<i>B. b. spinosus</i>	Iberian		JQ348596	JQ348739	JQ348485
11	DNA	42.6253	1.0864	Son	Spain	<i>B. b. bufo</i>	Iberian		JQ348573	JQ348716	JQ348528
12	DNA	38.7985	-9.3881	Sintra	Portugal	<i>B. b. spinosus</i>	Iberian		JQ348558	JQ348701	JQ348506
13	DNA	43.7206	3.1517	Serieys	France	<i>B. b. spinosus</i>	Iberian		JQ348602	JQ348745	
14	DNA	41.7600	2.3949	Montseny 1	Spain	<i>B. b. spinosus</i>	Iberian		JQ348549	JQ348692	JQ348522
15	DNA	41.7686	2.4699	Montseny 2	Spain	<i>B. b. spinosus</i>	Iberian		JQ348575	JQ348718	JQ348478
16	DNA	42.1858	-6.8684	Sanabria	Spain	<i>B. b. spinosus</i>	Iberian		JQ348559	JQ348702	JQ348503
17	DNA	43.1565	-3.8213	San Pedro del Romeral 1	Spain	<i>B. b. spinosus</i>	Iberian		JQ348579	JQ348722	JQ348491
18	DNA	43.1565	-3.8213	San Pedro del Romeral 2	Spain	<i>B. b. spinosus</i>	Iberian		JQ348580	JQ348723	JQ348496
19	DNA	43.8600	3.3807	Saint-Michel	France	<i>B. b. spinosus</i>	Iberian	BEV.1271-1272	JQ348547	JQ348690	JQ348481
20	DNA	36.0917	-5.4455	Riogetares	Spain	<i>B. b. spinosus</i>	Iberian		JQ348564	JQ348707	JQ348507
21	DNA	43.0995	-5.0109	Retuerto	Spain	<i>B. b. bufo</i>	Iberian		JQ348582	JQ348725	JQ348492
22	DNA	42.7154	-3.0592	Santa Gadea del Cid	Spain	<i>B. b. spinosus</i>	Iberian		JQ348562	JQ348705	JQ348488
23	DNA	43.0646	-5.3884	Puerto de San Isidro	Spain	<i>B. b. spinosus</i>	Iberian		JQ348590	JQ348733	JQ348490
24	DNA	40.9468	-3.7600	Puerto de Navacerrada	Spain	<i>B. b. spinosus</i>	Iberian		JQ348591	JQ348734	JQ348516
25	DNA	36.9166	-3.0423	Darrical	Spain	<i>B. b. spinosus</i>	Iberian		JQ348565	JQ348708	JQ348515
26	DNA	43.0107	-4.7463	Pozo de las Lomas	Spain	<i>B. b. bufo</i>	Iberian		JQ348600	JQ348743	JQ348523
27	DNA	43.0567	-3.8412	Penilla	Spain	<i>B. b. spinosus</i>	Iberian		JQ348583	JQ348726	JQ348493
28	DNA	44.8064	1.4554	Payrac	France	<i>B. b. spinosus</i>	Iberian	BEV.680	JQ348555	JQ348698	JQ348483
29	DNA	36.3649	-6.0718	Pago del Humo	Spain	<i>B. b. spinosus</i>	Iberian		JQ348567	JQ348710	JQ348525
30	DNA	47.5543	-1.6529	Nozay	France	<i>B. b. spinosus</i>	Iberian		JQ348601	JQ348744	JQ348504
31	DNA	43.5755	3.7195	Murviel-lès-Montpellier	France	<i>B. b. spinosus</i>	Iberian	BEV.682			JQ348415
32	DNA	43.2275	3.1938	Mire l'Etang	France	<i>B. b. spinosus</i>	Iberian	BEV.8851	JQ348684	JQ348689	
33	DNA	43.8867	3.5680	Rogues	France	<i>B. b. spinosus</i>	Iberian	BEV.1456		JQ348688	
34	DNA	43.0897	-1.3034	Luzaide	Spain	<i>ambiguous</i>	Iberian		JQ348589	JQ348732	JQ348499
35	DNA	37.8801	-6.6210	Linares de la Sierra	Spain	<i>B. b. spinosus</i>	Iberian		JQ348557	JQ348700	JQ348505
36	DNA	42.5652	2.1004	Les Angles	France	<i>B. b. spinosus</i>	Iberian		JQ348595	JQ348738	JQ348479
37	DNA	36.8343	-3.6744	Lentegi	Spain	<i>B. b. spinosus</i>	Iberian		JQ348568	JQ348711	JQ348520
38	DNA	42.3693	-8.000	Punxin	Spain	<i>ambiguous</i>	Iberian		JQ348577	JQ348720	JQ348502
39	DNA/allozymes	39.6667	-9.000	Pataias	Portugal	<i>B. b. spinosus</i>	Iberian		JQ348597	JQ348740	
40	DNA	43.5248	5.5470	Le Tholonet	France	<i>B. b. spinosus</i>	Iberian		JQ348553	JQ348696	JQ348480
41	DNA	43.0462	-1.0733	Larrau	France	<i>B. b. bufo</i>	Iberian		JQ348682	JQ348827	JQ348498
42	DNA	40.2841	-5.2497	Gredos 1	Spain	<i>B. b. gredosicola</i>	Iberian		JQ348592	JQ348735	JQ348512
43	DNA	40.2841	-5.2497	Gredos 2	Spain	<i>B. b. gredosicola</i>	Iberian		JQ348593	JQ348736	JQ348513
44	DNA	40.2841	-5.2497	Gredos 3	Spain	<i>B. b. gredosicola</i>	Iberian		JQ348569	JQ348712	JQ348511
45	DNA/allozymes	43.5547	2.7941	Lac du Saut de Vésoles	France	<i>B. b. spinosus</i>	Iberian		JQ348548	JQ348691	JQ348482
46	DNA	40.8640	-3.6156	La Cabrera	Spain	<i>B. b. spinosus</i>	Iberian		JQ348584	JQ348727	JQ348494
47	DNA	36.5444	-5.6616	24 km NE of medina-Sidonia	Spain	<i>B. b. spinosus</i>	Iberian		JQ348566	JQ348709	JQ348508
48	DNA	43.0556	-5.3261	Isoba	Spain	<i>B. b. bufo</i>	Iberian		JQ348586	JQ348729	JQ348495
49	DNA	42.8816	-0.7153	Lac d'Ansabère	France	<i>ambiguous</i>	Iberian		JQ348574	JQ348717	JQ348521
50	DNA	41.7867	1.2908	Guissona	Spain	<i>B. b. spinosus</i>	Iberian		JQ348588	JQ348731	JQ348489
51	DNA	37.6568	-5.5224	Lora del Rio	Spain	<i>B. b. spinosus</i>	Iberian		JQ348578	JQ348721	JQ348510
52	DNA	36.2767	-6.0884	Conil de la Frontera	Spain	<i>B. b. spinosus</i>	Iberian		JQ348587	JQ348730	JQ348519
53	DNA	43.9638	3.3232	Combe-Redonde	France	<i>B. b. spinosus</i>	Iberian		JQ348554	JQ348697	
54	DNA	42.4728	-7.9853	San Cristovo de Ceá	Spain	<i>ambiguous</i>	Iberian		JQ348551	JQ348694	JQ348476
55	DNA	36.9612	-3.3586	Capileira	Spain	<i>B. b. spinosus</i>	Iberian		JQ348594	JQ348737	JQ348509
56	DNA	42.3719	2.9221	Capmany	Spain	<i>B. b. spinosus</i>	Iberian		JQ348576	JQ348719	JQ348484

(continued on next page)

Table 1 (continued)

Specimen number	Data Type	Latitude	Longitude	Locality	Country	Taxon	Clade/MCA group	VOUCHER	GenBank RNA-16S 1 <sup>st</sup> part	GenBank16S 2 <sup>nd</sup> part	GenBank ND1
57	DNA	38.1479	-6.5601	Bodonal de la Sierra	Spain	<i>B. b. spinosus</i>	Iberian		JQ348572	JQ348715	JQ348518
58	DNA	43.0490	-1.6145	Puerto de Belate	Spain	<i>B. b. bufo</i>	Iberian		JQ348561	JQ348704	JQ348487
59	DNA	41.4501	2.2474	Badalona	Spain	<i>B. b. spinosus</i>	Iberian		JQ348552	JQ348695	JQ348477
60	DNA	39.3037	-0.5859	Catadau	Spain	<i>B. b. spinosus</i>	Iberian	BEV.7287	JQ348598	JQ348741	JQ348514
61	DNA	37.8744	-6.6661	Alajar	Spain	<i>B. b. spinosus</i>	Iberian		JQ348571	JQ348714	JQ348526
62	DNA	41.8077	-2.7856	Abejar	Spain	<i>B. b. spinosus</i>	Iberian		JQ348570	JQ348713	JQ348517
63	DNA	40.6996	39.4678	Anayurt	Turkey	<i>B. b. spinosus</i>	European	BEV.7627-7628	JQ348659	JQ348804	JQ348447
64	DNA	44.1167	15.2333	Zadar	Croatia	<i>B. b. spinosus</i>	European		JQ348657	JQ348802	JQ348456
65	DNA/ allozymes	45.400	29.600	Vilkovo	Ukraine	<i>B. b. bufo</i>	European		JQ348660	JQ348805	JQ348469
66	DNA	40.3796	15.5310	Teggiano	Italy	<i>B. b. spinosus</i>	European		JQ348648	JQ348793	JQ348466
67	DNA	43.3187	11.3305	Siena	Italy	<i>B. b. spinosus</i>	European		JQ348667	JQ348812	JQ348436
68	DNA	52.7066	1.3993	Wroxham	UK	<i>B. b. bufo</i>	European		JQ348661	JQ348806	JQ348445
69	DNA/ allozymes	39.6167	19.7833	Ropa, Kerkira island	Greece	<i>B. b. spinosus</i>	European		JQ348668	JQ348813	JQ348432
70	DNA	56.9465	24.1048	Riga	Latvia	<i>B. b. bufo</i>	European		AY325988		
71	DNA	41.4135	26.6289	Pythio	Greece	<i>B. b. spinosus</i>	European		JQ348658	JQ348803	JQ348446
72	DNA	46.0808	12.5378	Piancavallo	Italy	<i>B. b. spinosus</i>	European		JQ348622	JQ348767	JQ348458
73	DNA	40.3490	15.4383	Piaggine	Italy	<i>B. b. spinosus</i>	European		JQ348649	JQ348794	JQ348463
75	DNA	48.7406	22.4890	Perechin	Ukraine	<i>B. b. bufo</i>	European		JQ348636	JQ348781	JQ348438
76	DNA	36.6910	15.0692	Pachino	Italy	<i>B. b. spinosus</i>	European		JQ348654	JQ348799	JQ348474
77	DNA	40.0436	22.3002	Olympus mt.	Greece	<i>B. b. spinosus</i>	European		JQ348627	JQ348772	JQ348431
78	DNA	52.6281	1.2993	Norwich	UK	<i>B. b. bufo</i>	European		JQ348632	JQ348777	
79	DNA	43.7734	7.2241	Nice	France	<i>B. b. spinosus</i>	European	BEV.T2997	JQ348683		JQ348452
80	DNA	42.9244	12.0579	Monteleone d'Orvieto	Italy	<i>B. b. spinosus</i>	European		JQ348643	JQ348788	JQ348434
81	DNA	38.8723	23.2389	Marouli	Greece	<i>B. b. spinosus</i>	European		JQ348631	JQ348776	JQ348430
82	DNA	41.5516	13.1711	Maenza	Italy	<i>B. b. spinosus</i>	European		JQ348640	JQ348785	JQ348433
83	DNA	50.7635	4.27931	Lot	Belgium	<i>B. b. bufo</i>	European		JQ348665	JQ348810	JQ348470
84	DNA	51.0020	4.3019	Londerzeel	Belgium	<i>B. b. bufo</i>	European		FJ882806		
85	DNA	37.9208	13.3732	Lago Scanzano 1	Italy	<i>B. b. spinosus</i>	European		JQ348651	JQ348796	JQ348460
86	DNA	37.9208	13.3732	Lago Scanzano 2	Italy	<i>B. b. spinosus</i>	European		JQ348653	JQ348798	JQ348472
87	DNA	54.7333	49.2333	Kokryad	Russia	<i>B. b. bufo</i>	European		JQ348637	JQ348782	JQ348440
88	DNA	40.0764	22.2269	Kokkinopilos	Greece	<i>B. b. spinosus</i>	European		JQ348625	JQ348770	JQ348426
89	DNA	55.4580	12.1821	Køge	Denmark	<i>B. b. bufo</i>	European		JQ348635	JQ348780	JQ348437
90	DNA	39.6358	21.2182	Katafyto	Greece	<i>B. b. spinosus</i>	European		JQ348628	JQ348773	JQ348428
91	DNA	53.5757	7.9003	Jever	Germany	<i>B. b. bufo</i>	European		JQ348633	JQ348778	
92	DNA	57.1601	18.3362	Havdhem, Gotland	Sweden	<i>B. b. bufo</i>	European	BEV.7720	JQ348634	JQ348779	
93	DNA	36.9664	21.6989	Gialova	Greece	<i>B. b. spinosus</i>	European		JQ348626	JQ348771	JQ348427
94	DNA	44.5769	6.0532	Gap	France	<i>B. b. spinosus</i>	European	BEV.1259	JQ348672	JQ348817	JQ348443
95	DNA/ allozymes	49.65	36.26	Haidary	Ukraine	<i>B. b. bufo</i>	European	ZISP.7282	JQ348673	JQ348818	JQ348442
96	DNA	46.6468	6.0088	Foncine-le-Bas	France	<i>B. b. bufo</i>	European	BEV.8928	JQ348675	JQ348820	JQ348455
97	DNA	37.9871	14.9083	Floresta	Italy	<i>B. b. spinosus</i>	European		JQ348656	JQ348801	JQ348462
98	DNA	40.9272	37.9523	Kayabaşı	Turkey	<i>B. b. spinosus</i>	European	BEV.7656	JQ348679	JQ348824	JQ348449
99	DNA	39.5528	16.0222	Lago dei Due Uomini	Italy	<i>B. b. spinosus</i>	European		JQ348655	JQ348800	JQ348465
100	DNA	39.5604	21.3719	Desi	Greece	<i>B. b. spinosus</i>	European		JQ348630	JQ348775	JQ348429
101	DNA	45.2868	5.9067	Crolles	France	<i>ambiguus</i>	European	BEV.T2998	JQ348623	JQ348768	JQ348451
102	DNA	44.4722	9.0083	Creto	Italy	<i>B. b. spinosus</i>	European		JQ348642	JQ348787	JQ348471
103	DNA	45.7725	4.1759	Cleppé	France	<i>B. b. spinosus</i>	European	BEV.10226	JQ348624	JQ348769	
104	DNA	39.5167	15.9500	Cetraro	Italy	<i>B. b. spinosus</i>	European		JQ348686	JQ348763	JQ348464
105	DNA	37.8835	14.6564	Cesaro	Italy	<i>B. b. spinosus</i>	European		JQ348652	JQ348797	JQ348461
106	DNA	38.0825	14.8162	Castell'Umberto	Italy	<i>B. b. spinosus</i>	European		JQ348676	JQ348821	JQ348473
107	DNA	41.1260	16.8693	Bari	Italy	<i>B. b. spinosus</i>	European		JQ348650	JQ348795	JQ348467
108	DNA/ allozymes	41.6667	12.9833	Campa di Segni	Italy	<i>B. b. spinosus</i>	European	ZISP.9534	JQ348641	JQ348786	JQ348435
109	DNA	37.7597	13.8930	Caltavuturo 1	Italy	<i>B. b. spinosus</i>	European		JQ348685	JQ348762	JQ348459
110	DNA	37.7597	13.8930	Caltavuturo 2	Italy	<i>B. b. spinosus</i>	European		JQ348678	JQ348823	JQ348468
111	DNA	40.1833	28.8905	Bursa	Turkey	<i>B. b. spinosus</i>	European		DQ158438		
112	DNA	46.3667	14.1085	Bled	Slovenia	<i>ambiguus</i>	European		JQ348664	JQ348809	JQ348450
113	DNA	48.6	35.6	Balakhovka	Ukraine	<i>B. b. bufo</i>	European		JQ348638	JQ348783	JQ348441
115	DNA	41.5548	36.1127	Bafra	Turkey	<i>B. b. spinosus</i>	European	BEV.7635	JQ348671	JQ348816	JQ348448
116	DNA	47.2802	13.2313	Au	Austria	<i>B. b. bufo</i>	European		JQ348620	JQ348765	JQ348453
117	DNA/ allozymes	38.0333	23.7167	Athens	Greece	<i>B. b. spinosus</i>	European		JQ348629	JQ348774	JQ348475
118	DNA	45.9675	11.4142	Asiago	Italy	<i>ambiguus</i>	European		JQ348621	JQ348766	JQ348457
119	DNA	44.4742	3.8612	Altier	France	<i>B. b. spinosus</i>	European	BEV.10238	JQ348677	JQ348822	JQ348444
120	DNA	44.9298	4.8899	Valence	France	<i>B. b. spinosus</i>	European		JQ348663	JQ348808	JQ348454
121	DNA	41.65	41.80	Tirala Mt.	Russia	<i>B. verrucosissimus</i>	Caucasian	ZISP.6534	JQ348644	JQ348789	JQ348416

122	DNA/ allozymes	44.0833	40.7667	Psebai	Russia	<i>B. verrucosissimus</i>	Caucasian	ZISP.6547	JQ348647	JQ348792	JQ348424
123	DNA	41.8262	46.2697	Lagodekhi	Georgia	<i>B. verrucosissimus</i>	Caucasian	ZISP.4963	JQ348645	JQ348790	JQ348417
124	DNA	45.4167	40.6167	Kyurdzhinovo	Russia	<i>B. verrucosissimus</i>	Caucasian	ZISP.6541	JQ348619	JQ348764	JQ348420
125	DNA/ allozymes	44.7167	38.6833	Krepostnaya	Russia	<i>B. verrucosissimus</i>	Caucasian		JQ348662	JQ348807	JQ348425
126	DNA	42.9053	41.9833	Katkova	Georgia	<i>B. verrucosissimus</i>	Caucasian		JQ348670	JQ348815	JQ348423
127	DNA/ allozymes	41.7167	46.6	Katekh	Azerbaijan	<i>B. verrucosissimus</i>	Caucasian		JQ348674	JQ348819	JQ348418
128	DNA	44.83	40.20	Guzeripl	Russia	<i>B. verrucosissimus</i>	Caucasian	ZISP.6614	JQ348669	JQ348814	JQ348421
129	DNA	44.5777	38.0802	Gelenjik	Russia	<i>B. verrucosissimus</i>	Caucasian		JQ348646	JQ348791	JQ348422
130	DNA/ allozymes	38.45	48.73	Sim	Azerbaijan	<i>B. eichwaldi</i>	Caspian		JQ348681	JQ348826	JQ348546
131	DNA/ allozymes	38.65	48.8	Avrora	Azerbaijan	<i>B. eichwaldi</i>	Caspian	ZISP.7185	JQ348680	JQ348825	JQ348545
132	DNA	35.3689	-5.5402	Zinat	Morocco	<i>B. b. spinosus</i>	African		JQ348614	JQ348757	JQ348541
133	DNA	34	-4	Tazeka 1	Morocco	<i>B. b. spinosus</i>	African		JQ348608	JQ348751	JQ348535
134	DNA	34	-4	Tazeka 2	Morocco	<i>B. b. spinosus</i>	African		JQ348609	JQ348752	JQ348536
135	DNA	35.0706	-5.1742	3 km NE of Bab Taza	Morocco	<i>B. b. spinosus</i>	African		JQ348615	JQ348758	JQ348537
136	DNA	33.5161	-4.5322	Skoura M'daz	Morocco	<i>B. b. spinosus</i>	African		JQ348613	JQ348756	JQ348539
137	DNA	35.2801	-5.4018	Souk-el-Arba-des-Beni-Hassan	Morocco	<i>B. b. spinosus</i>	African		JQ348612	JQ348755	JQ348544
138	DNA	35.3335	-5.5382	Moulay Abdeslam	Morocco	<i>B. b. spinosus</i>	African		JQ348611	JQ348754	JQ348542
139	DNA	34.8759	-6.2495	Merja Zerga	Morocco	<i>B. b. spinosus</i>	African		JQ348617	JQ348760	JQ348540
140	DNA	34.05	-3.7667	Ifrane	Morocco	<i>B. b. spinosus</i>	African		JQ348618	JQ348761	JQ348538
141	DNA/ allozymes	34.95	-5.23	Fifi	Morocco	<i>B. b. spinosus</i>	African		JQ348607	JQ348750	JQ348533
142	DNA	35.1242	-5.7749	3 km W of Hamaimoun	Morocco	<i>B. b. spinosus</i>	African		JQ348610	JQ348753	JQ348534
143	DNA	32.4908	-5.2347	Tounfite	Morocco	<i>B. b. spinosus</i>	African		JQ348616	JQ348759	JQ348543
144	DNA/ allozymes	36.7304	8.7080	Ain Draham 1	Tunisia	<i>B. b. spinosus</i>	African	ZISP.7523	JQ348603	JQ348746	JQ348532
145	DNA	36.776	8.6917	Ain Draham 2	Tunisia	<i>B. b. spinosus</i>	African		JQ348606	JQ348749	JQ348531
146	DNA	36.7304	8.7080	Ain Draham 3	Tunisia	<i>B. b. spinosus</i>	African		JQ348605	JQ348748	
147	DNA	36.7801	8.8183	Ain Draham 4	Tunisia	<i>B. b. spinosus</i>	African		JQ348604	JQ348747	JQ348530
148	Allozymes	57.5833	9.9667	Hirtshals	Denmark	<i>B. b. bufo</i>	European	ZISP.8525-8526			
149	Allozymes	55.6833	13.1667	Lund	Sweden	<i>B. b. bufo</i>	European				
150	Allozymes	52.6000	13.6167	Blumberg	Germany	<i>B. b. bufo</i>	European				
151	Allozymes	45.5000	17.5167	1.5 km N of Mrkoplje	Croatia	<i>B. b. spinosus</i>	European				
152	Allozymes	54.7333	28.3333	Domzheritsy	Byelorussia	<i>B. b. bufo</i>	European				
153	DNA/ allozymes	54.38	20.64	Bagrationovsk	Russia	<i>B. b. bufo</i>	European	ZISP.7048	JQ348639	JQ348784	JQ348439
154	Allozymes	59.56	30.12	Gatchina	Russia	<i>B. b. bufo</i>	European	ZISP.6992, 7259, 7508			
155	Allozymes	59.45	29.37	6 km W Volosovo	Russia	<i>B. b. bufo</i>	European				
156	Allozymes	61.50	29.98	Ikhala	Russia	<i>B. b. bufo</i>	European				
157	Allozymes	55.60	40.67	Gus-Khrustalnyi	Russia	<i>B. b. bufo</i>	European				
158	Allozymes	54.2167	37.6167	Tula	Russia	<i>B. b. bufo</i>	European				
159	Allozymes	51.48	23.85	Svityaz'	Ukraine	<i>B. b. bufo</i>	European				
160	Allozymes	50.43	25.74	Dubno	Ukraine	<i>B. b. bufo</i>	European				
161	Allozymes	48.7833	29.5167	Chechelivka	Ukraine	<i>B. b. bufo</i>	European				
162	Allozymes	46.65	29.75	Laptura Lake	Moldavia	<i>B. b. bufo</i>	European				
163	Allozymes	36.6948	-5.7733	San Jose del Valle	Spain	<i>B. b. spinosus</i>	Iberian				
165	Allozymes	35.4920	-5.8227	5 km NE of Charkia	Morocco	<i>B. b. spinosus</i>	African				
166	Allozymes	40.6167	31.2833	Abant Lake	Turkey	<i>B. b. spinosus</i>	Caucasian	ZISP.8101-8103			
167	DNA/ allozymes	36.55	32.1167	Alanya	Turkey	<i>B. b. spinosus</i>	Caucasian		JQ348666	JQ348811	JQ348419
168	Allozymes	42.98	41.10	Bagmaran	Abkhazia	<i>B. verrucosissimus</i>	Caucasian				
169	Allozymes	43.17	40.35	Lidzava	Abkhazia	<i>B. verrucosissimus</i>	Caucasian				
170	Allozymes	43.80	40.65	Nikitino	Russia	<i>B. verrucosissimus</i>	Caucasian				

## OUTGROUPS

Species	Locality	Country	Data Type	GenBank ref
<i>B. gargarizans</i>	Chusan Island	China	DNA	NC008410.1
<i>B. gargarizans</i>	Song	China	DNA	FJ882843.1
<i>B. gargarizans</i>	Bonevurovka	Russia	allozymes	Allozymes - 171
<i>B. gargarizans</i>	Krym	Russia	allozymes	Allozymes - 172
<i>B. gargarizans</i>	Novoaleksandrovsk (Sakhalin Island)	Russia	allozymes	Allozymes - 173
<i>B. gargarizans</i>	Quingcheng Mt. (Sichuan Province)	China	allozymes	Allozymes - 174
<i>B. japonicus</i>	Hiroshima	Japan	DNA	NC009886.1
<i>B. andrewsi</i>	Yunnan	China	DNA	FJ882808

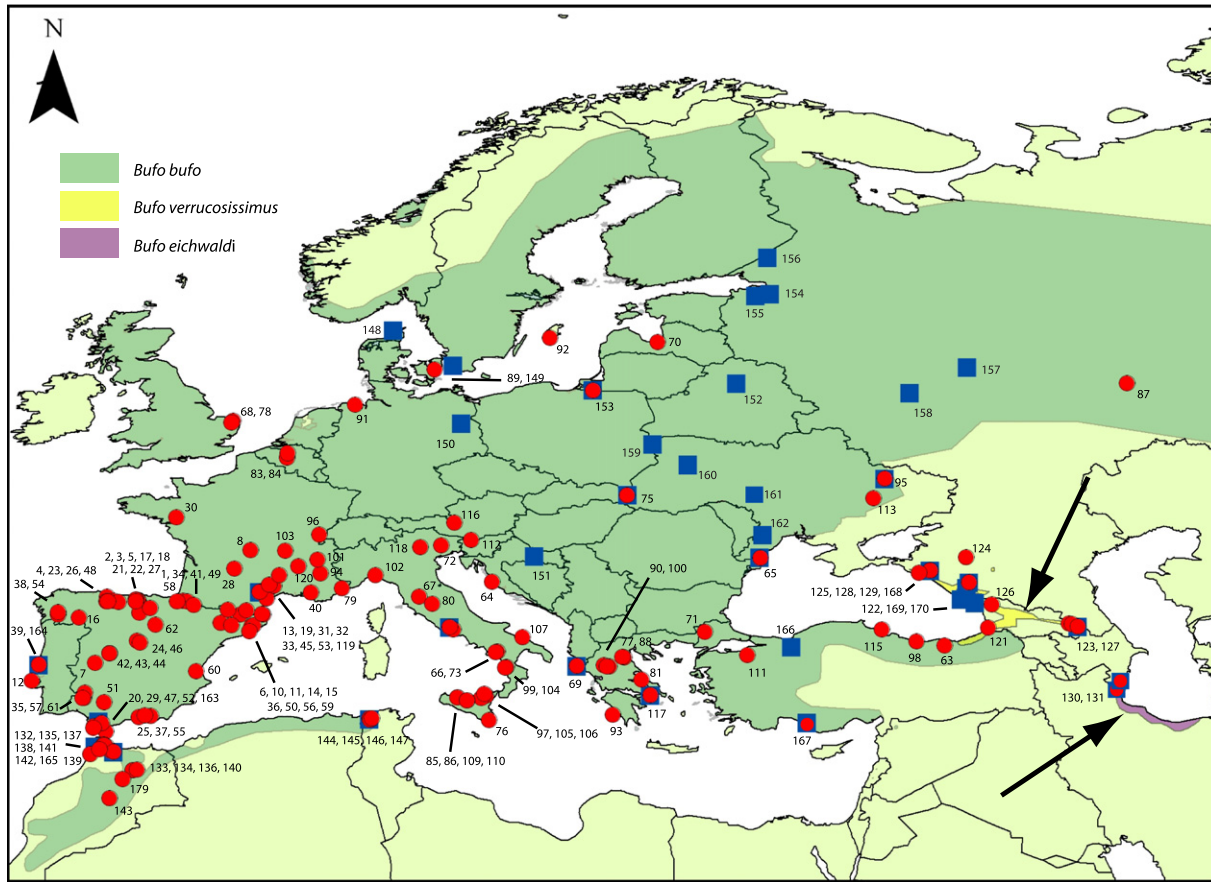


**Fig. 1.** Sampling localities included in the present study. Red circles indicate DNA sampling localities; blue squares indicate allozyme sampling localities. The background colors indicate the known distribution of *Bufo bufo* (green), *Bufo verrucosissimus* (yellow) and *Bufo eichwaldi* (purple). Map numbers refer to specimens listed in Table 1 and Fig. 2. Arrows highlight the distribution ranges of *B. verrucosissimus* and *B. eichwaldi*. (For interpretation of the references to color in this figure legend, the reader is referred to the web version of this article.)

for the ML and Bayesian analyses under Akaike's information criterion. This was the GTR model taking into account the gamma distribution and the number of invariant sites for each of the two independent partitions. To explore the topological space, we performed 1000 independent heuristic searches each one starting from a parsimony tree. The likelihoods of the resulting trees of each run were compared and the one with the highest  $-\log L$  was selected. Reliability of the ML searches was assessed by bootstrap analysis (Felsenstein, 1985), involving 1000 replications. Support values for every node were superimposed onto the best tree topology.

BI analysis was conducted using MrBayes 3.1.2 (Ronquist and Huelsenbeck, 2003). The dataset was split into the same two partitions mentioned before (protein-coding and RNA-coding mitochondrial regions) and two independent runs of four Markov chain Monte Carlo (MCMC) chains were executed in parallel for 10 million generations, with a sampling interval of 1000 generations. Preliminary analyses (data not shown) revealed that our dataset was extremely sensitive to the branch-length prior, producing trees with very long branches (several orders of magnitude longer than the branches of the ML tree). This is not a rare phenomenon, which has been reviewed and analyzed in several recent papers (e.g. Brown et al., 2010; Marshall, 2010). To solve this problem, we followed the recommendations by Brown et al. (2010) and specified a branch-length prior with a smaller mean to reduce the posterior probability of the long-tree region in the branch-length space. The new mean was calculated using the formula proposed by the authors and was set to 1/379. Convergence of the two runs was evidenced by a split frequency standard deviation

lower than 0.01 and by potential scale-reduction factors to 1 for all model parameters as shown by the command "sump" in MrBayes (Ronquist and Huelsenbeck, 2003). Posterior probabilities (pp) for every clade were obtained by combining the sampled trees from the two parallel runs excluding a relative burn-in of 30% of the trees from each run. In both analyses three species of the *Bufo gargarizans* species complex were used to root the tree (*Bufo gargarizans*, *Bufo japonicus* and *Bufo andrewsi*).

To determine whether the mtDNA data supported the currently established taxonomic partitions proposed by Mertens and Wermuth (1960), we used topological constraints to enforce monophyly of the subspecies as currently defined (see Table 1), using the package Mesquite v2.78 (Maddison and Maddison, 2009). Topological constraints were compared to optimal topologies using the Approximately-Unbiased (AU) (Shimodaira, 2002) and Shimodaira-Hasegawa tests implemented in CONSEL (Shimodaira and Hasegawa, 2001). The subspecies were assigned to our specimens following Mertens and Wermuth (1960), Lizana (2002) and Muratet (2008) and on information on the morphological variation of the species (PAC and PG, unpublished results). The specimens of dubious taxonomic assignment were excluded from the test.

### 2.3. Allozymes

Sixteen protein systems, corresponding to 21 presumptive loci were examined for 172 specimens from 40 different localities, including *Bufo gargarizans* and representatives from all the species

and subspecies of the *Bufo bufo* species complex, with the only exception of *B. b. gredosicola*. Electrophoretic conditions for the proteins studied were as described by Litvinchuk et al. (2008). The populations of the *Bufo bufo* species complex included in the allozyme analysis are shown in Fig. 1, and the corresponding locality names and taxonomic assignment are presented in Table 1.

The software BIOSYS-1 (Swofford and Selander, 1981) was used to calculate the average expected and observed heterozygosity per locus (Hexp and Hobs), the percentage of polymorphic loci (P), as well as Nei's genetic distances (Nei, 1978). The matrix of Nei's genetic similarities was converted into a neighbor-joining tree (NJ; Saitou and Nei, 1987) using MEGA 5.0 (Tamura et al., 2011). This method of phylogenetic reconstruction is known to perform well for allozyme data (Wiens, 2000).

A Multiple Correspondence Analysis (MCA) on the population frequency data was performed with the computer software Statistica Kernel version 5.5 (StatSoft, Inc.; Tulsa, USA). For this analysis each row in the dataset was a population and each column represented the frequency of the *i*th allele of the *j*th locus.

#### 2.4. Dating estimates

Divergence dates for our dataset were estimated using a Bayesian relaxed molecular clock approach (BRMC) by means of the package BEAST v. 1.5.2 (Drummond and Rambaut, 2007). Given that some priors (e.g. tree priors) do not adequately account simultaneously for both interspecific (phylogenetic priors) and intraspecific data (coalescent priors), we opted for a reduction of our dataset maintaining solely one representative of each clade as appeared in our ML phylogeny. In this way we also reduced the amount of intraspecific polymorphism, which yields an overestimation of the divergence times when deep and external calibration points are used (Ho et al., 2008).

In order to introduce the calibration points, all external to our ingroup, we included the *Bufo bufo* species complex in the phylogenetic context of 173 species belonging to the family Bufonidae (approximately 30% of the species of the family) plus six species that were used as outgroups (Supplementary material I and II).

Four external calibration points were used, all of them already employed in previous studies to calibrate timescales encompassing the whole family Bufonidae (Pramuk et al., 2007; Van Bocxlaer et al., 2009, 2010, see references therein) (Supplementary material II):

1. A soft maximum of 49 Ma for the split between the Caribbean Bufonidae (genus *Peltophryne*) and their closest mainland relatives (genus *Rhaebo*). This calibration is based on the geological evidence implying that the existence of emerged land in the Caribbean Sea is not older than 37–49 Ma. The soft maximum was obtained by means of a lognormal distribution with a mean placed in 27 Ma, a standard deviation of 0.35 and an offset of 5 Ma.
2. The oldest fossil attributable to the family Bufonidae in North America (20 Ma), was used as a minimum age for the split between the North American toads (genus *Anaxyrus*) and their sister group, the Central-American toads of the genus *Incilius*. This was set using a gamma distribution ( $\alpha = 1.2$ ,  $\beta = 4$ ) starting at 20 Ma.
3. The oldest fossils belonging to the *Bufo viridis* species complex, all dating from the Lower Miocene of Southeastern France, Greece, Northern Turkey and Southern Germany, are assumed in this study to belong to the lineage leading to the European *Bufo viridis* complex, therefore representing a minimum age for the split between this lineage and the lineage leading to *Bufo surdus*. The calibration point was associated to a Gamma distribution ( $\alpha = 1.2$ ,  $\beta = 4$ ) with an offset placed in 18 Ma.

4. The oldest fossil attributable to the *Rhinella marina* species complex (11 Ma), was established as a minimum age for the split between the *Rhinella marina* species complex and its sister group, the *Rhinella granulosa* species complex. This was set by means of a Gamma distribution ( $\alpha = 1.2$ ,  $\beta = 4$ ) with an offset established in 11 Ma.

Preliminary analyses showed that our mitochondrial markers (*tRNAval*, *16S* and *ND1*) could not resolve deep nodes, so we concatenated two nuclear genes *CXCR4* (688 pb) and *NCX1* (1285 pb) downloaded from GenBank to improve the resolution of the deep splits (see Supplementary material I). The unalignable regions of the noncoding mitochondrial markers were removed by means of Gblocks (Castresana, 2000), eliminating the misaligned regions and the positions with more than 50% missing data (36% of the original mitochondrial dataset).

A Yule branching process with a uniform prior and an uncorrelated branch rate variation was modeled by means of a resampling from a lognormal distribution. The model of evolution was set to GTRGAMMAI. The clock model and the evolutionary models were applied independently to the four partitions: (1) mitochondrial protein-coding; (2) mitochondrial RNA-coding; (3) nuclear *CXCR4*; and (4) nuclear *NCX1* (Van Bocxlaer et al., 2009).

The analysis consisted of five independent Markov chain Monte Carlo (MCMC) analyses; each chain was run for 25,000,000 generations with parameters and trees sampled every 1000 generations. These five independent runs converged on very similar posterior estimates and were combined using LogCombiner version 1.4 after excluding the first 5,000,000 generations in each one (Rambaut and Drummond, 2007). Tracer 1.2 (Rambaut and Drummond, 2007) was used to confirm convergence and good mixing of the five combined MCMC chains. Finally we generated the maximum clade credibility consensus tree with median node heights using the TreeAnnotator program (also included in BEAST package), setting the posterior probability limit to 0.5.

#### 2.5. Species distribution modeling

Distribution models were used to tackle two questions: first, to test the role of the Central Asian Deserts as a biogeographic barrier; and secondly to examine whether the climate-based potential distribution of the species in the Last Glacial Maximum (LGM) could explain the shallow structure found in the most structured parts of our phylogeny.

##### 2.5.1. Testing the Central Asian Deserts as a biogeographic barrier

Correlative distribution models can be very useful tools for testing the existence of environmental barriers to dispersal and gene flow, particularly when we suspect, as in this case, that the distribution limits can be greatly determined by climatic causes (the existence of the Central Asian Deserts) (Kozak et al., 2008; Sexton et al., 2009).

To accomplish this, we modeled the current distribution of both species complexes in Eurasia. The *Bufo bufo* species complex was modeled using the localities included in this study (168 localities) to which we added 269 georeferenced localities of the species complex in Russia and adjacent countries (unpublished data from SNL) plus 23,803 localities from its entire distribution range obtained from Gbif (<http://data.gbif.org>). To produce the distribution models of the *Bufo gargarizans* species complex, we downloaded from Gbif all available localities of *Bufo tibetanus* (511 localities), *Bufo andrewsi* (1959 localities), *Bufo tuberculatus* (9 localities), *Bufo cryptotypanicus* (4 localities) and *Bufo gargarizans* (787 localities). The localities belonging to *Bufo japonicus* (18 localities) were obtained from Igawa et al. (2006).

The models were generated by Maxent 3.3.1 (Phillips et al., 2006; Phillips and Dudík, 2008). To avoid highly correlated and redundant climatic variables in our climatic dataset, which can cause over-parametrization and loss of predictive power (Williams et al., 2003; Buermann et al., 2008), the environmental data from 10,000 randomly generated points from across the study area were extracted and, from there, the level of correlation between pairs of variables was analyzed using the Pearson correlation coefficient. When two variables shared a correlation coefficient of 0.80 or higher, these were considered highly correlated, and the most meaningful variable was selected according to the physiological requirements of a typical mesophilic amphibian. Following this criterion, of the 19 variables available, eight variables were retained as input data for the distribution models: Bio1 (annual mean temperature), Bio2 (mean diurnal range), Bio7 (temperature annual range), Bio8 (mean temperature of wettest quarter), Bio12 (annual precipitation), Bio13 (precipitation of the wettest period), Bio15 (precipitation seasonality) and Bio18 (precipitation of the warmest quarter).

We generated models for each species complex independently and models pooling the localities of both species complexes. In both cases, we generated eight sets of 50 replicates of the distribution models, every set with increasing regularization values (1, 3, 5, 9, 20, 30, 40 and 50). By doing so, we progressively reduced the overfitting of our data in every replicate, producing more spread-out potential distributions (Phillips et al., 2006). The rationale is to extend as much as possible the distribution of both species complexes in all possible directions to test the stability of the Central Asian Deserts as a biogeographic barrier. Convergence threshold and maximum number of iterations corresponded to default settings of the program (0.00001, 500 respectively). For each set, we considered the mean of the 50 models the best estimate for the potential limits for both species. Model performance was evaluated using the AUC and the threshold-dependent binomial omission tests calculated by Maxent.

#### 2.5.2. Testing the effects of glaciations

We explored whether the range shifts and population fragmentation experienced by the species during the Late Quaternary (0.0117–0.126 Ma) were congruent with the shallow phylogenetic structure of the European–Caucasian clade (the clade with the highest degree of geographic structure, see results). Localities corresponding to the European–Caucasian clade were projected onto the current climate and, assuming niche stability during the last 18,000 years (Nogués-Bravo, 2009), onto two possible reconstructions of the climatic conditions during the last glacial maximum (LGM), which were based on two models: the Community Climate System Model (CCSM) and the Model for Interdisciplinary research on Climate (MIROC). The climatic layers from the current and past scenarios were downloaded from the WorldClim (<http://www.worldclim.org>) database at 2.5° spatial resolution. The methodology used to generate the layers can be found in Waltari et al. (2007) and Hijmans et al. (2005).

Both present-day and past distribution models were generated through 100 replicates with Maxent 3.3.1 (Phillips et al., 2006; Phillips and Dudík, 2008) using the same climatic layers previously selected. To the 89 georeferenced localities of the European–Caucasian clade obtained by ourselves, we added 30 localities selected from Gbif (<http://www.gbif.org>) to cover the less-sampled areas. In each replicate, 70% of the localities were used to train the model and 30% to test it. The model calibrated with the present-day occurrence data was projected onto the current climate and past climatic conditions. Convergence threshold, maximum number of iterations, regularization values and features were set to default values. The output probability of presence of the species was set to logistic, and a threshold of the 10th percentile of training presence

was used to generate binary layers. Finally, the binary maps of both models were superimposed by means of the program ArcMap v.9.3. The model performance was evaluated using the AUC and the threshold-dependent binomial omission tests calculated by Maxent.

### 3. Results

#### 3.1. Patterns of mitochondrial sequence variation and phylogeographic structure

The resulting mitochondrial dataset contained 1988 bp of which 289 bp were variable and 245 parsimony-informative (excluding the outgroups). The phylogenetic tree resulting from the analysis of the mitochondrial data is presented in Fig. 2 and reveals five major haplotype clades with the following geographic delimitations (see Figs. 2 and 3): (1) Caspian clade, the basal-most split within the *Bufo bufo* species complex, corresponding to the species *Bufo eichwaldi*. It is distributed along the Southern shore of the Caspian Sea (Southeastern Azerbaijan and probably Iran); (2) European clade, corresponding to *Bufo bufo* sensu stricto (includes specimens from the type locality of *Bufo bufo*). According to Fig. 2 and Table 1, this clade appears to include specimens classified as both *B. b. bufo* and *B. b. spinosus*. It is the sister group to the Caucasian clade and is the clade with the largest distributional range, encompassing most of the currently known distribution of the species with the exception of Southern and Western France, Iberian Peninsula, North Africa and the Caucasus; (3) Caucasian clade, the sister group to the European clade, includes the taxon *Bufo verrucosissimus* and one population (locality 167) assigned to *B. b. spinosus* (Table 1). It is distributed across the Caucasus, with one population in Anatolia; (4) Iberian clade, distributed across the entire Iberian Peninsula and Southern and Western France, includes populations classified as *B. b. spinosus* and *B. b. gredosicola*; and (5) African clade, the sister group to the Iberian clade, includes specimens assigned to *B. b. spinosus* only and it is distributed across the mountain ranges and humid areas of Morocco, Algeria and Tunisia.

The average uncorrected sequence divergence ( $p$ -distance) among these five major clades is 5.42%. Table 2 shows the pairwise distances among clades for the 16S and ND1 genes.

As stated above, *Bufo b. spinosus* and *B. b. bufo* were not monophyletic in our analyses of the mtDNA data (Fig. 2 and Table 1). The results of both the SH and AU tests indicate that the best tree enforcing monophyly of the currently defined subspecies has significantly less likelihood ( $P < 0.0001$ ) than the unconstrained ML topology shown in Fig. 2 ( $\text{Log}L_{\text{unconstrained}} = -7570.303$ ;  $\text{Log}L_{\text{constrained}} = -8034.871$ ).

Regarding the shallow phylogenetic structure, the different clades show different degrees of intraclade structuring. The Iberian clade does not have a well-supported structure in either ML or BI analyses, and this structure lacks correlation with geography (Figs. 1 and 2). By contrast, the European, Caucasian and African clades show an explicit degree of geographic structuring in both ML and BI analyses. Indeed, in the European clade seven subclades are recovered in our analysis, corresponding to the following geographic regions (see Figs. 2 and 3): Southern Italy (e7), North-Central Italy (e6), Greek Peninsula (e5), North-Central Europe (e1), South-Central Europe (e3), Southwestern Europe (e2) and Anatolia (including Northeastern Greece) (e4). All of them have high pp and bootstrap support values with the only exception of the Anatolian clade (despite being recovered by both ML and Bayesian analyses).

In addition, the Caucasian clade is composed of three well-supported subclades: North Caucasus, South Caucasus and Central Anatolia (c1, c2 and c3 respectively), and the African clade includes two subclades, a Moroccan clade and a Tunisian clade (a1 and a2 respectively). The lack of sampling in Algeria hampers resolution

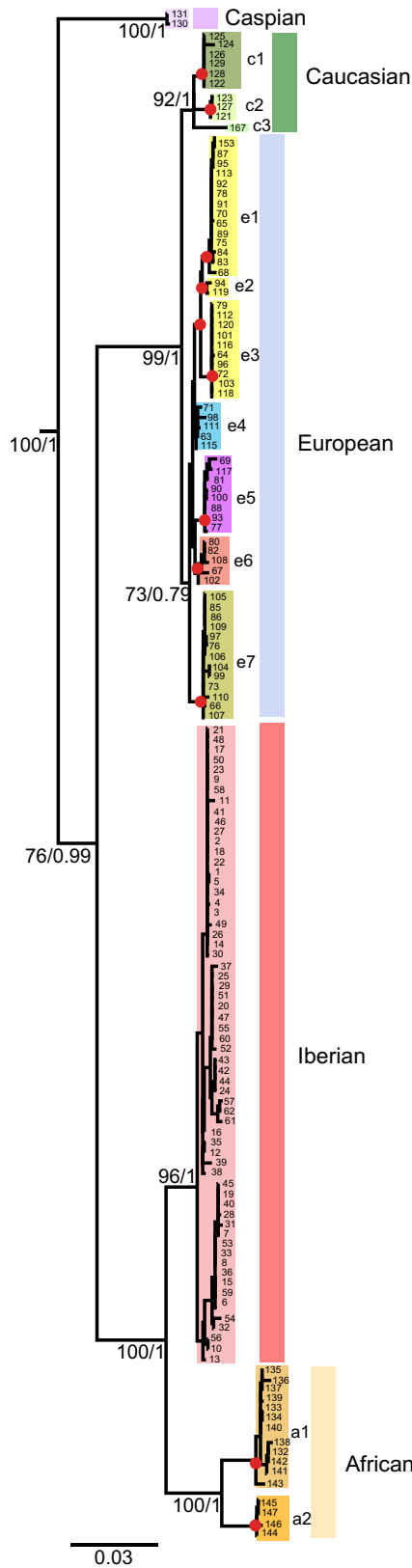


**Fig. 2.** Phylogenetic relationships of the *Bufo bufo* species complex in the Western Palearctic, as inferred from the ML analysis of 1988 bp of mtDNA. The support values (bootstrap/pp) are shown next to the nodes of the major splits. The red dots depicted in the shallow splits denote a bootstrap value equal or higher than 80% and simultaneously a posterior probability equal or higher than 0.90. The reference bar is expressed in substitutions per site. Numbers at the tips of the tree refer to specimens listed in Table 1. The outgroups have been removed. (For interpretation of the references to color in this figure legend, the reader is referred to the web version of this article.)

of the precise geographic contact between these two clades. The Moroccan clade presents some genetic differentiation between the population from the Great Atlas and the populations from the Rif/Middle Atlas.

3.2. Allozymes

Allele frequencies, sample size, percentage of polymorphic loci, and average heterozygosity are presented in Supplementary material III. Among 21 presumptive loci, 16 are polymorphic and include between two and seven alleles. The MCA analysis of allozyme variation is presented in Fig. 4. The populations are grouped according to the five mtDNA clades (Fig. 2) and not according to the current taxonomy (see Table 1). Specimens from localities 69, 108 and 117 (Table 1), classified as *B. b. spinosus*, in fact present mtDNA and allozymes of *B. b. bufo*, while specimens from localities 166 and 167, also classified as *B. b. spinosus*, group with *B. verrucosissimus*. Based on the fact that multiple independent nuclear loci are more likely to reflect evolutionary history than the mitochondrial locus, the six main mtDNA clades thus seem to correspond to the real evolutionary history of the *Bufo bufo* species complex. However, the NJ tree (Fig. 4c) based on Nei's genetic distances among populations (Supplementary material IV) does not recover the African and Iberian populations as monophyletic.

A number of populations occupy an intermediate position in the MCA scatter plots (Fig. 4a and b) and exhibit a mix of alleles typical of more than one lineage (Supplementary material III; see also Supplementary material V for scores along the first four axes for the MCA analyses). The Greek populations 69 and 117 have an intermediate position between the Caucasian and European groups, and it is clearly not an artifact, as these populations exhibit a mix of Caucasian and European alleles, indicating mixed ancestry of the Greek populations (Supplementary material III). The single individual analyzed from locality 108 (Italy) carries mostly European alleles, confirming its assignment based on mtDNA (Fig. 2), but it also presents at two loci (*Est-3*, *G6pdh*) Iberian alleles that are not found in any other individual of the Caucasian or European populations. Specimens from another locality (locality 45; Lac du Saut de Vésoles, S. France) occupy an intermediate position in the MCA scatter plots between the European and Iberian clades (Fig. 4). Its mtDNA places it with the Iberian clade, but its nuclear DNA exhibits both European and Iberian alleles (Supplementary material III). Both the Caspian and Caucasian populations are well separated in the MCA analysis.

The average Nei's genetic distances among the five clades are shown in Supplementary material VI. All the clades are genetically very well differentiated (Nei's genetic distance: 0.196–0.632). The lower genetic distance corresponds to the comparison between the Caucasian and European clades and the highest to the comparison between the Caucasian and African clades. The European populations sampled for the allozyme study (see Fig. 1 and Table 1) present a low level of genetic differentiation (average Nei's genetic distance: 0.010), despite being from localities as far away as Denmark, Sweden, Germany, Croatia, Russia, Belarus, Moldova and Ukraine. In contrast, the Moroccan and Tunisian populations of the African mtDNA clade are genetically very distinct (Nei's genetic distance: 0.349). This value is comparable to the genetic distance between the Iberian and African populations (see Supplementary material VI) and supports the distinctiveness of these three lineages obtained in the mtDNA phylogenetic analysis.

3.3. Dating estimates

Our BRMC calibrated ultrametric tree for all Bufonidae yielded most of the clades compatible with previously published phyloge-

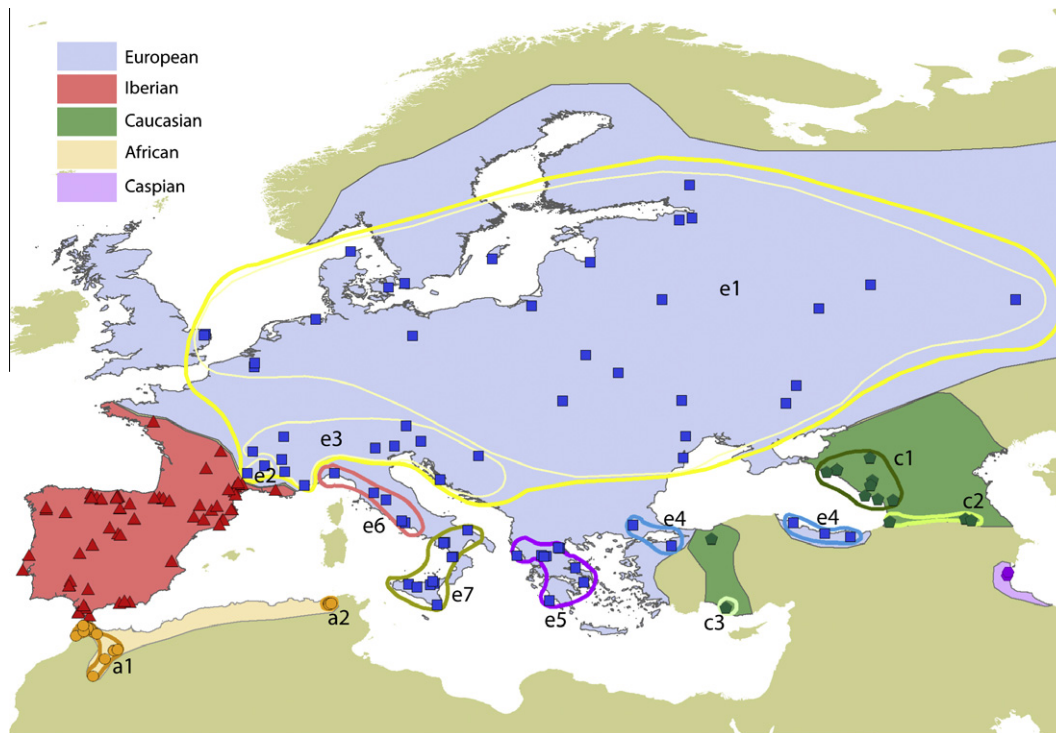


**Fig. 3.** Map showing the geographic distribution of the major clades (mitochondrial) and MCA groups (allozymes) recovered in our analyses (background colors). The outlines depict the shallow phylogenetic structure. The colors and codes have correspondence with those employed in Fig. 2 and in the text. Morocco (a1), Tunisia (a2), North-Central Europe (e1), Southwestern Europe (e2), South-Central Europe (e3), Anatolia (including Northeastern Greece) (e4), Greek Peninsula (e5), North-Central Italy (e6), Southern Italy (e7), North Caucasus (c1), South Caucasus (c2), Central Anatolia (c3). (For interpretation of the references to color in this figure legend, the reader is referred to the web version of this article.)

**Table 2**

Estimates of evolutionary divergence over sequence pairs between clades in terms of the number of base differences per site (*p*-distance) from averaging over all sequence pairs. Upper right, distances for the 16S; lower left, distances for the ND1.

Clades	Caucasian	European	Iberian	African	Caspian
Caucasian	–	0.009	0.041	0.049	0.038
European	0.034	–	0.043	0.050	0.039
Iberian	0.100	0.093	–	0.034	0.047
African	0.096	0.093	0.054	–	0.057
Caspian	0.116	0.117	0.095	0.099	–

nies of this family (Van Bocxlaer et al., 2009, 2010), and all the nodes involving the *Bufo bufo* species complex were recovered with the highest possible support (posterior probability of 1) (Supplementary material II).

The crown age of the family Bufonidae was estimated at approximately 60 Ma (95% HDP = 47.94–75.48 Ma), compatible with previous estimates (Roelants et al., 2007; Van Bocxlaer et al., 2009, 2010) and with the age of the oldest fossil attributable to the family Bufonidae (55 Ma old) (Báez and Nicoli, 2004).

Regarding our ingroup (Fig. 5), the age of the split between the *Bufo bufo* and the *Bufo gargarizans* species complexes was estimated at 12.33 Ma (95% Highest Posterior Density = 8.81–16.36 Ma). The separation between *Bufo eichwaldi* and the main European populations occurred approximately 7.42 Ma (95% HPD = 5.15–9.99 Ma) and was followed by the split between the ancestor of the European and Caucasian populations and the ancestor of the Iberian and African populations, which occurred around 5.21 Ma (95% HPD = 3.67–7.11 Ma). Finally, our dating estimates place the separation between the Iberian and the African populations at 3.07 Ma (95% HPD = 1.91–4.36 Ma), with the remaining splits occurring within the Pleistocene (Fig. 5).

### 3.4. Distribution modeling

#### 3.4.1. The Central Asian Deserts as a biogeographic barrier

All distribution models of both species complexes across Eurasia produced either independently or pooled provided mean AUC values beyond 0.9 and significance for all binomial omission tests, indicating a good performance of the models (data not shown). As shown in Fig. 6, although suitable climatic conditions for both species complexes seem to exist along the Himalayan range, implying a possible contact zone, the genus *Bufo* has never been reported in this region, which instead is occupied by the Indian-radiated genus *Duttaphrynus* and the widespread Palearctic genus *Bufotes* (Van Bocxlaer et al., 2009; Frost, 2011). Therefore, excluding this predicted contact zone, the distributions of both species complexes appear to be disjoint and nowadays completely isolated by the hyperarid, arid and semiarid regions of Central Asia. This pattern of isolation between both species complexes was resilient to the increase of the regularization values from 1 to 50, although each increment of the value produced more spread-out distributions.

#### 3.4.2. Glaciations as drivers of phylogeographic structure

Modeling of distribution of populations of the European mtDNA clade yielded, on the current climate conditions, a mean test AUC score of 0.856, and all thresholds measured by the binomial omission tests were significantly nonrandom (data not shown). A visual inspection of the predicted distribution under the current climatic conditions showed overall an adequate fit to the distributions of the species as presented in Gasc et al. (1997) (data not shown).

The distribution models based on the LGM conditions indicate a substantial southward retraction of the ranges for the European

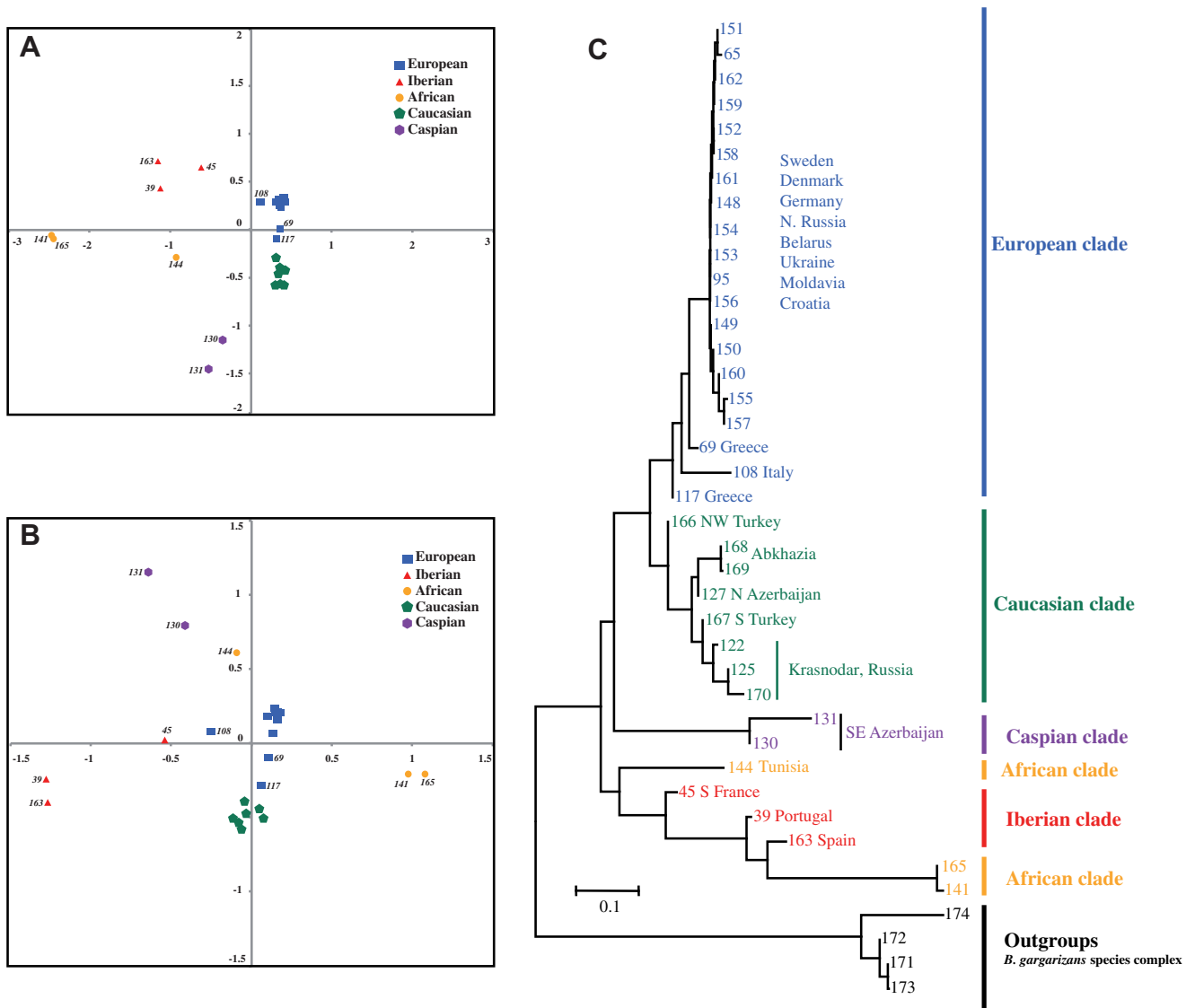


**Fig. 4.** Multiple Correspondence Analysis (MCA) of *Bufo* populations and neighbor-joining tree based on Nei's genetic distances among populations based on allozyme data. Data on the allozyme frequencies can be found in Supplementary material III. Information on the specimens analyzed can be found in Table 1 and their geographic position is shown in Fig. 1. (A) Biplot of factor 1 and 2 scores of the MCA analysis; (B) biplot of factors 3 and 4 of the MCA analyses. Scores along the first four axes for the MCA analyses can be found in Supplementary material V. (C) Neighbor-joining tree. The colors and codes have correspondence with those employed in Figs. 2 and 3. (For interpretation of the references to color in this figure legend, the reader is referred to the web version of this article.)

clade, with no suitable climate predicted above 53° of latitude in Central Europe (Fig. 7). The extent of range shrinkage is variable depending on the climatic model, being more severe under the CCSM and more relaxed under the MIROC. In both cases all Mediterranean Peninsulas, Anatolia and Caucasus appear suitable with different degrees of range fragmentation depending on the model. A substantial area in central Europe appears to be appropriate for the species according to the MIROC model.

#### 4. Discussion

##### 4.1. The role of the Central Asian Deserts as a biogeographic barrier

Our calibrated timetree sets the age of the split between *Bufo bufo* and *Bufo gargarizans* species complexes around 12.33 Ma (95% Highest Posterior Density = 8.81–16.36 Ma), and this is compatible with the oldest fossil attributable to the genus *Bufo* sensu stricto. This fossil from Suchomasty (Czech Republic) was dated to the MN9 (11.1–9.7 Ma) by Rage and Roček (2003),

although Mein (1999), based on mammal faunas, assigned the locality to the MN10 (9.7–8.7 Ma) (Agustí et al., 2001).

Our distribution models (Fig. 6) show that both species complexes are completely isolated by the arid areas of Central Asia, a result congruent with a scenario of a climate-driven isolation between these two species complexes assuming niche conservatism during the last 10 My. However, our estimate of 12.33 Ma for the timing of this vicariant event (Fig. 5) does not match the most recent geological studies based on Loess deposits in China, which show that the Central Asian inland deserts originated in the Early Miocene, 22 Ma (Guo et al., 2008) or even 24 Ma (Sun et al., 2010). Despite that, the event that separated these two species complexes was probably not the geological origin of the Central Asian Deserts but their emergence as biogeographic barriers, and these two phenomena do not necessarily have to be synchronous. In fact, mineralogical and sedimentological records of the Northern-South China Sea show that the aridification process of Central Asia was not a homogeneous process but encompassed several pulses of accelerated aridification, with two great pulses at approx-

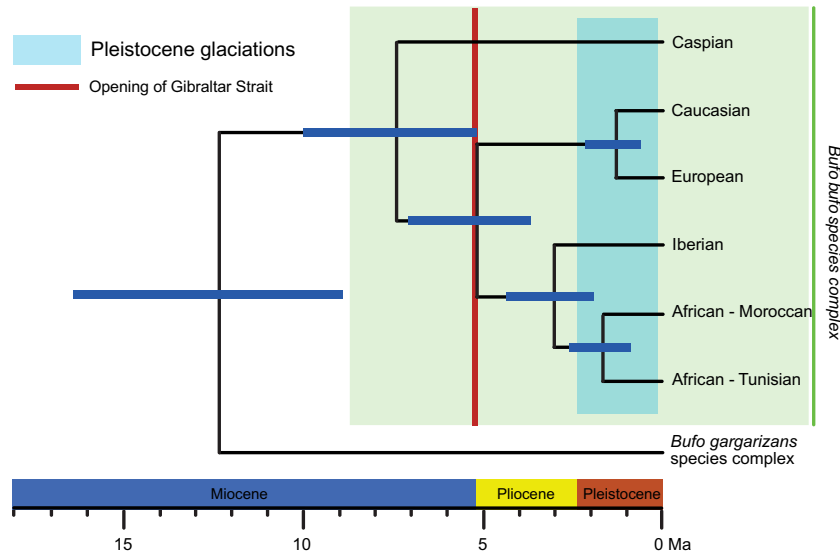


**Fig. 5.** Enlarged view of the Bayesian time-calibrated tree (Supplementary material II) showing the divergence times within the *Bufo bufo* species complex. The horizontal bars indicate the 95% posterior age intervals.

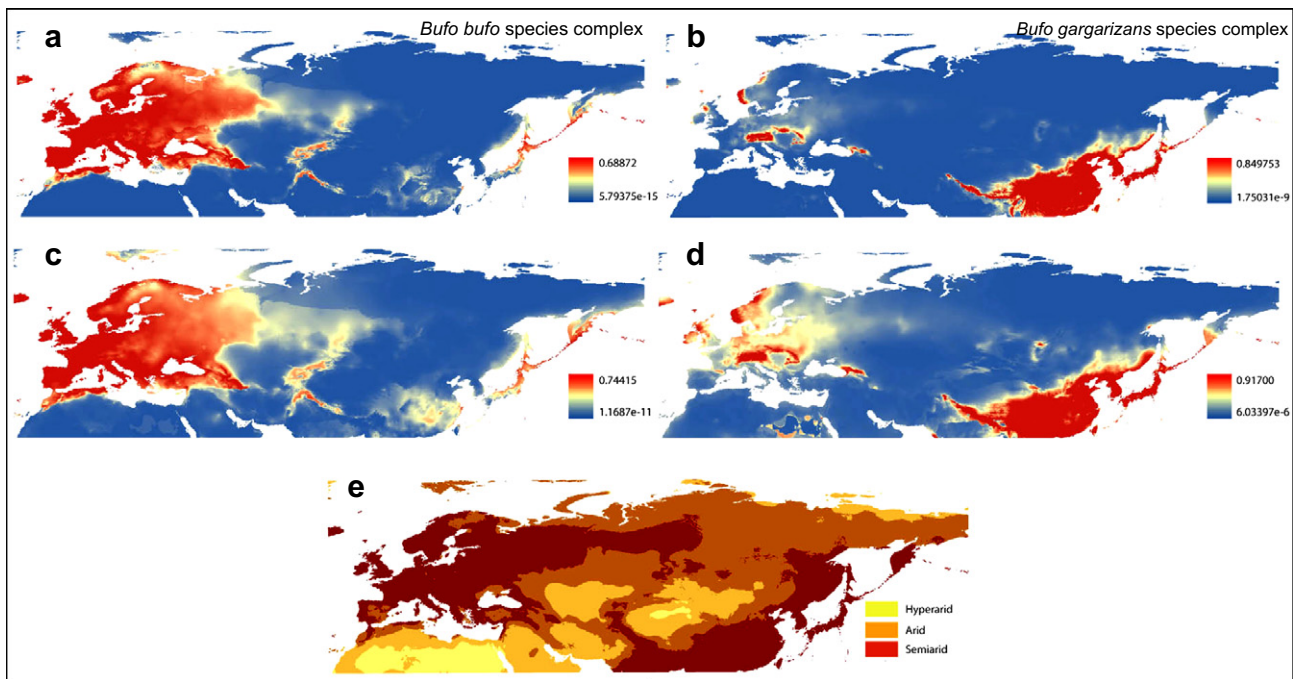


**Fig. 6.** Potential distribution of the *Bufo bufo* species complex and the *Bufo gargarizans* species complex across Eurasia, with different regularization factors: *a* and *b* = 9, *c* and *d* = 50. The map *e* shows the current extent of the desertic and subdesertic areas in Central Asia. The color gradient next to each map indicates the predicted probability that environmental conditions are suitable for the species. (For interpretation of the references to color in this figure legend, the reader is referred to the web version of this article.)

imately 15 and 8 Ma (Wan et al., 2007). This estimate matches those of several studies from widely separated places in the Eastern part of China's Loess Plateau, which show initial accumulation of loess between 10–8 Ma (Donghuai et al., 1998; Ding et al., 1999; Qiang et al., 2001).

From a paleobiological perspective, major levels of mean hypsodonty (dentition characterized by high-crowned teeth, typical of species inhabiting arid habitats) are observed in the large mammal faunas of Central China during the early Late Miocene (11.1–9.7 Ma), indicating an increase in aridity during this time interval (Liu et al., 2009). Moreover, the palynological record of the North-eastern margin of Tibet also reflects a marked shift towards more

arid landscapes around 9 Ma (Ma et al., 1998; Sun and Wang, 2005).

Other diversification events fully agree with the development of the Central Asian Deserts during the Middle Miocene (15.9–11.6), either as an effective biogeographic barrier or as a source of new habitats that enhanced arid-adapted species radiations. An example of the latter is the origin of the radiation of desert-adapted lizards of the genus *Phrynocephalus* which, for Central Asia, dates between 17 and 11 Ma (Melville et al., 2009), according to the existing overlap of the 95% HPD between the estimates of the mitochondrial and nuclear markers. Moreover, the dating of the split between the Eastern and Western species complexes of *Bombina*,

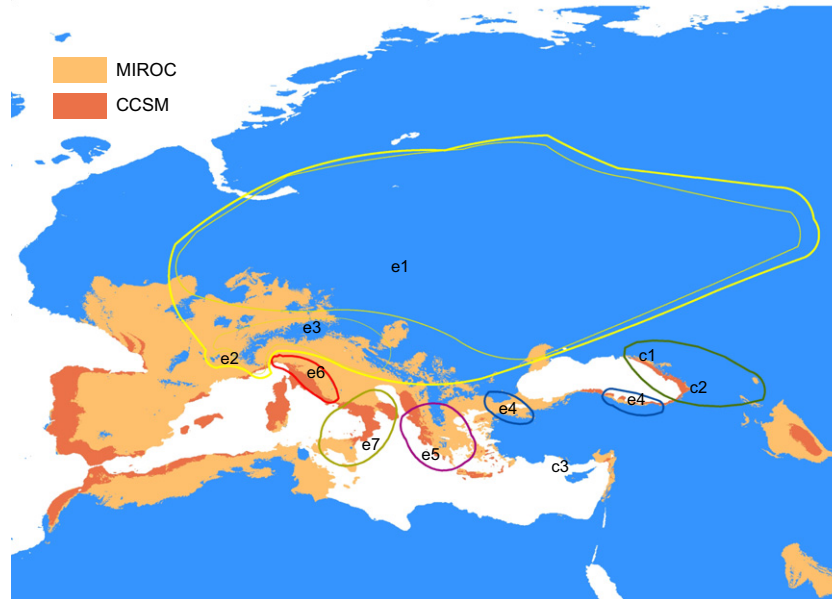


**Fig. 7.** Potential distribution of the European–Caucasian clade on two paleoclimatic scenarios during the LGM: MIROC (light orange) and CCSM (dark orange). The outlines represent the internal structure of the European–Caucasian clades. The colors and codes of the outlines have correspondence with those employed in Figs. 2 and 3. (For interpretation of the references to color in this figure legend, the reader is referred to the web version of this article.)

another case of Central Asian vicariance, has been established between 13.8 and 6.6 Ma (Roelants et al., 2007) and between 20.9 and 5.1 Ma (Zheng et al., 2009). These values are also compatible with our dating estimates.

All this evidence points to the complete isolation of lineages triggered by an increase in the arid conditions in the Central Asian region, supporting a climate-driven isolation between Eastern and Western species complexes as proposed by Savage (1973) and Borkin (1984).

#### 4.2. Major splits in the Western Palearctic

Between the Late Miocene and Early Pliocene (11.6–3.6 Ma) two successive splits occurred: the separation of the lineage leading to *Bufo eichwaldi* (Caspian clade) from the rest and the separation between the ancestor of the European and Caucasian populations and the ancestor of the Iberian and African populations (Fig. 5). Several other cladogenetic events in amphibians have been reported in Europe within the same temporal frame: *Bombina bombina/Bombina variegata* (Fromhage et al., 2004), *Triturus vulgaris/Triturus montandoni* (Zajc and Arntzen, 1999), *Pelophylax fortis/Pelophylax ridibundus* (Akin et al., 2010), *Hyla arborea/Hyla orientalis* (Stöck et al., 2008a,b), and possibly the Eastern and Western lineages of *P. fuscus* (Crottini et al., 2007). The existence of the Paratethys Sea following an Eastern–Western axis in Central–Eastern Europe during the Miocene has been proposed to explain the split between the snakes, *Natrix natrix* and *Natrix tessellata* (Guicking et al., 2006), as a consequence of a North–South vicariance. This same vicariance could also explain the divergence between the Caspian population from the remaining populations of the *Bufo bufo* species complex given that the Paratethys Sea partially isolated what are now the Caucasus and the Southern Caspian shore from the rest of Europe during the Late Miocene (Popov et al., 2006).

However, the Late Miocene is also a period of a severe climatic and ecological reorganization already initiated around 10 Ma, when the European continent progressively shifted from more or less homogeneous humid conditions to drier conditions with higher levels of climatic and ecological heterogeneity. In fact, the Middle Turolian (7.6–6.8 Ma) is a period of upsurge of dry and open

habitats as can be deduced from the great expansion of the savanna-adapted Pikermian faunas (Solounias et al., 1999) and the paleopalynologic record (fossil pollen and spores) (Fauquette et al., 2006). However it is between the Middle and Late Turolian (7–5 Ma) when the major break in climatic conditions occurred according to the levels of mammalian hypsodonty, with a transient phase of strong aridity dominating a large part of continental Europe (Fortelius et al., 2002, 2006; Van Dam, 2006). We hypothesize that this paleoclimatic scenario is congruent with severe changes in the population ranges of mesophilic amphibians, which eventually could lead to cladogenetic events.

#### 4.3. Overseas dispersal across the Strait of Gibraltar and North African genetic structure

According to our mtDNA phylogenetic results (Fig. 2), North Africa was colonized from the Iberian Peninsula. Our dating estimates place the split between the Iberian and African clades clearly after the reopening of the Gibraltar Strait, implying overseas dispersal (Fig. 5). So far, this same mode of dispersal has been proposed for some mammals (Cosson et al., 2005), many reptiles (Carranza et al., 2004; Carranza et al., 2006; see Pleguezuelos et al., 2008 for a review), some invertebrates (e. g. Horn et al., 2006) and, regarding amphibians, it has been suggested for some lineages of *Pleurodeles waltl* (Veith et al., 2004; Carranza and Arnold, 2004; Carranza and Wade, 2004) and *Hyla meridionalis* (Recuero et al., 2007), although in both cases human-mediated dispersal cannot be fully excluded. In the Mediterranean basin, overseas dispersal from Africa to Europe has been suggested for the *Bufo viridis* species complex (Stöck et al., 2008b).

The dispersal capabilities of amphibians across the sea have been evidenced several times despite the apparent severe limitations that salt water imposes to their physiology (Measey et al., 2007; Vences et al., 2003). Some of the best known events of overseas dispersal by amphibians seem to be mediated by the combination of two factors: (1) great rivers able to expel islets of soil and vegetation a long way into the open sea; and (2) long-persisting torrential rains that can greatly reduce the salinity across the oceanic dispersal path (Measey et al., 2007). Although during the Pli-

ocene Western Europe was overall wetter than today (Jost et al., 2009), probably rains were never intense enough to produce a substantial decrease in seawater salinity. However great Iberian rivers, such as the Guadalquivir, could have had an important role in projecting rafts into the open water, which afterwards could have reached the North African coast through the currents. In the particular case of *Bufo bufo*, it is known that brackish waters do not prevent animals from swimming in open water in the North Baltic Sea, even allowing gene flow between islands (Seppa and Laurila, 1999), indicating a certain degree of salt tolerance in this species.

The African group comprises two highly supported subgroups corresponding to Moroccan versus Tunisian populations (Figs. 2–4), although in the NJ tree from Fig. 4c the African group is not monophyletic. This same pattern of high level of genetic variability in North Africa has been observed in several other groups, as for instance the lacertid lizard *Timon tangitanus*/*Timon pater* (Paulo et al., 2008), the frogs *Hyla meridionalis* (Recuero et al., 2007; Stöck et al., 2008a) and *Pelophylax saharicus* (Harris et al., 2003), the toad *Discoglossus scovazzi*/*Discoglossus pictus auritus* (Zangari et al., 2006), and the snakes *Natrix maura* (Guicking et al., 2006), *Natrix natrix* and *Coronella girondica* (pers. observ.). The arid conditions of the Moulouya Basin could explain this dichotomy, as evidenced by the gap in the potential distribution of the *Bufo bufo* species complex in North Africa (results not shown). However, because of our lack of samples in the wide area existing between our Easternmost Moroccan samples and our Tunisian samples (mainly Algeria), we cannot know with certainty whether the Moulouya Basin represents the vicariant event that separated these populations.

#### 4.4. Effects of glaciations

The Caucasian populations comprise three distinct subgroups (c1–c3; Fig. 2) and the European populations up to seven subgroups (e1–e7; Fig. 2). According to our dating estimates (Fig. 5) this structuring occurred during the Pleistocene and can be interpreted as signatures of the Quaternary glacial events, implying several cycles of retraction/expansion of the population ranges accompanied by strong effects of sorting of ancestral polymorphisms (Hewitt, 2000). The nested pattern observed in the European–Caucasian group suggests that at least two heterochronous events shaped its inner structure. The first event could have involved the Caucasian region as Pleistocene refugia, although we cannot exclude the possibility of an extra-Caucasian split with a posterior population retraction into the Caucasus. Secondary glacial events produced the youngest fragmentations, which, based on their strong geographic association, suggest that up to seven refugia could have existed (Figs. 2, 3 and 7).

The Caucasus appears in many phylogeographies as a source of distinctive lineages, involving cases of recent glacial-driven splits (Grassi et al., 2008). Paleopalynological data indicate the presence of a mild climate in the area during the LGM, as can be inferred from the presence of conifer and mixed forests in the Western Caucasus 18 Ka (Tarasov et al., 2000). This is congruent with our LGM projections that show the area as climatically suitable for the species and greatly isolated, supporting the hypothesis that it could have acted as a Pleistocene refugium (Fig. 7).

The structuring of the European populations is congruent with the existence of four Pleistocene refugia in the Mediterranean region and three refugia in Central Europe (see Figs. 2, 3 and 7). The Mediterranean refugia encompass Southern Italy (e7), Central/Northern Italy (e6), Greece (e5) and Anatolia (e4), and all of them have been reported as Pleistocene refugia for many groups, conforming to the Adriatic–Mediterranean and Pontic–Mediterranean elements based on chorological analysis (Schmitt, 2007). The existence of more than one phylogroup in the Italian Peninsula is a very common pattern in other Mediterranean Peninsulas,

revealing so-called “refugia within refugia” (Gómez and Lunt, 2007). The main phylogeographic feature found in many Italian taxa is the presence of distinctive lineages in the Sicilian–Southern Italian region, as observed for instance in the mammal *Sciurus vulgaris* (Grill et al., 2009), reptiles *Hierophis viridiflavus* and *Zamenis longissimus*/*Zamenis lineatus* (Joger et al., 2010) and amphibians *Bombina pachypus* (Canestrelli et al., 2006) and *Hyla intermedia* (Canestrelli et al., 2007). Our results match this pattern, with a clearly differentiated Southern Italian haplotype group distributed across Sicily and Southern Italy.

The genetic differentiation of the South Italian biotas has been attributed to two major physiographic features in the region, the Crati–Sibari graben and the Catanzaro graben, which have been repeatedly marine-flooded following glacio-eustatic sea-level fluctuations during the Upper Pliocene and Pleistocene, interrupting or reducing the genetic exchange with the rest of the Italian Peninsula (Santucci and Nascetti, 1996; Canestrelli et al., 2007; and references therein). However, considering the patchy distribution pattern observed in our climatic projection under the CCSM paleoclimatic scenario, we do not exclude a climatically driven isolation during the Pleistocene glaciations.

The Anatolian refugium was already suggested for *Bufo bufo* by Kutrup et al. (2006), and this is consistent with our Anatolian haplotype group, which is distributed from the Eastern Balkans–Western Anatolia to Eastern Anatolia (e4; Figs. 2 and 3). A similar phylogeographic pattern occurs in the reptile *Zamenis longissimus* (Joger et al., 2010) and several species of mammals (Randi, 2007; and references therein). The presence of a cool temperate forest has been proposed for a narrow band along the southern shore of the Black Sea 18 ka (Adams and Faure, 1997), supporting the putative role of this region as a glacial refugium.

Three subclades can be geographically associated with Central Europe, all of them phylogenetically closely related (see Figs. 2, 3 and 7): a South-Central European clade (e3) including Southern France, the Alpine region and Northern Balkans, a North-Central European clade (e1) encompassing Great Britain, Scandinavia, the North-Central European mainland reaching Western Russia and Ukraine, and a Southwestern European clade (e2) containing the localities of Gap and Altier in Southwestern France. Clades tightly associated with Central Europe have been reported for many groups. In the case of amphibians, these have been noted for *Rana arvalis* (Babik et al., 2004), *Rana temporaria* (Palo et al., 2004) and even in thermophilous species such as *Epidalea calamita* (Rowe et al., 2006). These phylogeographic patterns suggest the existence of Northern “cryptic” refugia for several species, and the existence of these refugia has been unambiguously corroborated on the basis of paleopalynology, paleontology (Stewart and Lister, 2001) and paleoclimatic modeling (Svenning et al., 2008). Our niche projection onto the MIROC paleoclimatic scenario indicates that suitable LGM climatic conditions could have existed across Central Europe for the European populations, supporting the possibility that the Central European populations could correspond to Northern “cryptic” refugia for the species; however, we cannot exclude the possibility that these populations could have originated from refugia located in the Northern Balkans (North-Central European clade) or the submediterranean areas of South-Central Europe (Southwestern and South-Central European clades), which also contained suitable areas for the species during the LGM according to our paleoclimatic projection (Fig. 7).

In the Iberian Peninsula, the Iberian populations fail to show a clear phylogeographic pattern, and this agrees with a previous genetic survey of Iberian populations using microsatellites and the mitochondrial control region revealing little population differentiation and extensive gene flow at a wide spatial scale (Martinez-Solano and Gonzalez, 2008). This suggests that the Iberian populations did not experience a great amount of population

fragmentation during the Pleistocene glaciations, possibly as a consequence of a single and wide Pleistocene refugium preserving a great amount of haplotypic diversity with little geographic fragmentation.

#### 4.5. Implications for the systematics of the *Bufo bufo* species complex

Although a subspecies or species is not necessarily monophyletic for mtDNA haplotypes, when monophyly of mtDNA haplotypes characterizes a geographic population, that observation serves as a strong diagnostic criterion for a historically distinct lineage. The results of both mtDNA and allozyme analyses support the same five main population lineages within the *Bufo bufo* species complex but do not show congruence with the currently accepted taxonomy of the group. The monophyly tests performed with the mtDNA data set clearly rejected monophyly of *Bufo bufo spinosus* and *Bufo bufo bufo* as currently defined (see above). The three samples of *Bufo b. gredosicola* included in the mtDNA study branched within *B. b. spinosus* from the Iberian haplotype clade. However, further studies including morphology, fast-evolving nuclear markers and a better sampling at the population level are needed to assess the taxonomic validity of the population of *Bufo bufo* from the Sierra de Gredos (Lizana, 2002). Populations assigned to *B. bufo spinosus* based on their morphology and geographic distribution presented mtDNA and/or allozymes typical of *B. b. bufo* (Greece and Italy: localities 69, 108 and 117; Table 1; Figs. 1, 2 and 4) or *Bufo verrucosissimus* (Western Anatolia, localities 166 and 167; Table 1; Figs. 1, 2 and 4). *Bufo b. spinosus* is traditionally diagnosed mainly based on its body size and the degree of development of the keratinous warts. Our results suggest that these characters evolved independently multiple times towards the Peri-Mediterranean area, possibly as an adaptation to dry environments. The relationship between moisture and size has been proposed by Duellman and Trueb (1994), with larger animals having greater desiccation tolerance due to the decrease in body surface (especially so in “spherical” shapes like the toads). Moreover, the level of keratinization could be related to desiccation tolerance as well.

Based on the mtDNA and allozymic results, each one of the five main population lineages of the *Bufo bufo* species complex represent a different taxon. According to the phylogeny from Fig. 2 and the taxonomy of the group, the Caspian population should be recognized at the specific level as *Bufo eichwaldi*. The results of the MCA analyses (Fig. 4) and a close inspection of the allozyme frequency table (Supplementary material III) clearly show that some of the populations present a mixed ancestry indicating extensive past or ongoing introgression. For instance, Greek populations 69 and 117, which carry mtDNA of the European haplotype clade (Fig. 2), have an intermediate position between the Caucasian populations and the European populations in the MCA allozyme analysis (Fig. 4). The same occurs with specimens from locality 108, assigned to the European population based on their mtDNA but with some Iberian alleles at some loci (*Est-3*, *G6phd*; see Fig. 4 and Supplementary material III), or with specimens from locality 45, classified as belonging to the Iberian population based on their mtDNA but with European alleles in some loci (Fig. 4; Supplementary material III). As a result of the observed introgression between the different populations and until a more detailed study reveals the contact zones, we prefer to regard the Caucasian, European, Iberian and African populations as different subspecies of *Bufo bufo*. Moreover, any future analyses should attempt to add information on the morphology and bioacoustics of the different populations.

Based on the information on the type localities, the name *Bufo bufo verrucosissimus* should be used for the Caucasian population, *Bufo bufo bufo* for the European population, *Bufo bufo spinosus*

should be restricted to the Iberian population and, until a new subspecies is described, *Bufo bufo ssp.* should be used for the African population. This latter population might, in fact, include two different subspecies, one in the Western Maghreb and another one in the Eastern Maghreb.

## 5. Conclusions

According to our results, the *Bufo bufo* and the *Bufo gargarizans* species complexes diverged during the Middle Miocene, most probably as a consequence of a climate-driven isolation coincident with an increase in the aridification of Central Asia. After this split between Eastern and Western complexes, at least three main lineages were generated within the *Bufo bufo* complex: (1) Caspian lineage (*Bufo eichwaldi*); (2) the Iberian-African lineage; and (3) the European-Caucasian lineage (Fig. 2). All these three splits were unambiguously placed in Pre-Pleistocene times according to our dating estimates, probably in the Late Miocene. We propose here that the cladogenetic events leading to these lineages could be mediated by the combination of paleogeographic features (as the Parathetys Sea) and the climate shift that occurred in Europe in the Late Miocene towards major levels of aridity and savanna-like environments.

A dispersion event leading to the colonization of Northern Africa occurred during the Pliocene, after the opening of the Gibraltar Strait, and this could be the first unambiguous case of overseas dispersal across the Gibraltar Strait for an amphibian.

The structure of the European-Caucasian populations involved at least two major reorganizations during the Pleistocene, with an older split between the European lineage and the Caucasian lineage, possibly involving the Caucasus as a Pleistocene refugium, and other shallower structuring mediated by more recent Pleistocene glaciations. These promoted high levels of geographic fragmentation and genetic differentiation in the European and Caucasian lineages. This more recent structuring is compatible with the range fluctuations experienced by Palearctic faunas during the Pleistocene concomitant to glacial events. We propose seven Pleistocene refugia, four Mediterranean refugia involving the Iberian and Italian peninsulas, the South Balkanic region and Anatolia, and three refugia with diffuse locations that together form an extensive Central European group (see Figs. 2, 3 and 7). These latter refugia were the most probable source for the recolonization of northern Europe after the ice withdrew. In contrast, the Iberian Peninsula seems not to have any structure coupled with geography, and this is probably the consequence of a single wide refugium retaining great amounts of ancestral polymorphism.

## Acknowledgments

The following persons contributed greatly in some part of the process of this study, either during the fieldtrips, lab part or either reading the manuscript and providing helpful improvements: Kim Roelants, Franky Bossuyt, An Mannaert, Wim Vandeborgh, Ines van Bocklaer, Ignasi Castellvi, Juan G. Renom, Isaac Casanovas-Vilar, Jose Castresana, Victor Soria-Carrasco, Alejandro Sanchez-Gracia, Emma Duran Alsina, Pere Garcia-Porta, Miquel A. Arnedo, Pedro Abellán, Mar Comas, Daniel Escoriza, David Donaire, Grégory Deso, Alexandre Teynié, Philip de Pous, Diego Alvarado-Serrano, Josep Roca and Javier Igea. The first author is recipient of a pre-doctoral research fellowship (JAE) from the CSIC. The work was partially funded by Grants CGL2008-00827 and CGL2009-11663 from the Ministerio de Educación y Ciencia, Spain to SC. S.N. Litvinchuk was partly supported by Grants NSH-3299.2010.4 and MCB-N22n. Comments by the Editor and two anonymous reviewers improved the manuscript.

## Appendix A. Supplementary material

Supplementary data associated with this article can be found in the online version, at doi:10.1016/j.ympev.2011.12.019.

## References

- Adams, J.M., Faure, H. (Eds.), 1997. QEN Members. Review and Atlas of Palaeovegetation: Preliminary Land Ecosystem Maps of the World since the Last Glacial Maximum. Oak Ridge National Laboratory, TN, USA. <<http://www.esd.ornl.gov/projects/qen/adams1.html>>.
- Agustí, J., Cabrera, L., Garces, M., Krijgsman, W., Oms, O., Pares, J.M., 2001. A calibrated mammal scale for the neogene of Western Europe. State of the art. Earth-Sci. Rev. 52, 247–260.
- Akin, Ç., Bilgin, M., Bilgin, C.C., 2010. Discordance between ventral colour and mtDNA haplotype in the water frog *Rana (ridibunda) caralitana* Arkan, 1988. Amphibia-Reptilia 31, 9–20.
- Azanza, B., Alberdi, M.T., Prado, J.L., 2000. Large mammal turnover pulses correlated with latest Neogene glacial trends in the northwestern Mediterranean region. Geol. Soc. London (Special Publications) 181, 161–170.
- Babik, W., Branicki, W., Sandera, M., Litvinchuk, S., Borkin, L.J., Irwin, J.T., 2004. Mitochondrial phylogeography of the moor frog, *Rana arvalis*. Mol. Ecol. 13, 1469–1480.
- Babik, W., Branicki, W., Crnobrnja-Isailović, J., Cog, D., Lniceanu, A., Sas, I., Olgun, K., Poyarkov, N.A., Garcia-Paris, M., Artzen, J.W., 2007. Phylogeography of two European newt species-discordance between mtDNA and morphology. Mol. Ecol. 14, 2475–2491.
- Báez, A.M., Nicoli, L., 2004. Bufonid toads from the Late Oligocene beds of Salla, Bolivia. J. Vertebr. Paleontol. 24, 73–79.
- Benson, D.A., Karsch-Mizrachi, I., Lipman, D.J., Ostell, J., Wheeler, D.L., 2008. GenBank. Nucleic Acid Research 36 (Database issue), D25–30.
- Biju, S.D., Bossuyt, F., 2003. New frog family from India reveals an ancient biogeographical link with the Seychelles. Nature 425, 711–714.
- Blondel, J., Aronson, J., 1999. Biology and Wildlife of the Mediterranean Region. Oxford University Press, Oxford.
- Borkin, L.J., 1984. The European-Far Eastern disjunctions in distribution of amphibians: a new analysis of the problem. Proc. Zool. Inst. Leningrad 124, 55–88.
- Brown, J.M., Hedtke, S.M., Lemmon, A.R., Lemmon, E.M., 2010. When trees grow too long: investigating the causes of highly inaccurate Bayesian branch-length estimates. Syst. Biol. 59, 145–161.
- Buermann, W., Saatchi, S., Smith, T.B., Zutta, B.R., Chaves, J.A., Mila, B., Graham, C., 2008. Predicting species distributions across the Amazonian and Andean regions using remote sensing data. J. Biogeogr. 35, 1160–1176.
- Canestrelli, D., Cimmaruta, R., Costantini, V., Nascetti, G., 2006. Genetic diversity and phylogeography of the Apennine yellow-bellied toad *Bombina pachypus*, with implications for conservation. Mol. Ecol. 15, 3741–3754.
- Canestrelli, D., Verardi, A., Nascetti, G., 2007. Genetic differentiation and history of populations of the Italian treefrog *Hyla intermedia*: lack of concordance between mitochondrial and nuclear markers. Genetica 130, 241–255.
- Carranza, S., Arnold, E.N., 2004. History of West Mediterranean newts, *Pleurodeles* (Amphibia: Salamandridae), inferred from old and recent DNA sequences. Syst. Biodivers. 1, 327–337.
- Carranza, S., Wade, E., 2004. Taxonomic revision of Algero-Tunisian *Pleurodeles* (Caudata: Salamandridae) using molecular and morphological data. Revalidation of the taxon *Pleurodeles nebulosus* (Guichenot, 1850). Zootaxa 488, 1–24.
- Carranza, S., Arnold, E.N., Pleguezuelos, J.M., 2006. Mitochondrial DNA indicates the Mediterranean snakes, *Malpolon monspessulanus* and *Hemorrhois hippocrepis* (Squamata, Colubridae), are recent colonizers of the Iberian Peninsula. Mol. Phylogenet. Evol. 40, 532–546.
- Carranza, S., Arnold, E.N., Wade, E., Fahd, S., 2004. Phylogeography of the false smooth snakes, *Macroprotodon* (Serpentes, Colubridae): mitochondrial DNA sequences show European populations arrived recently from Northwest Africa. Mol. Phylogenet. Evol. 33, 523–532.
- Castresana, J., 2000. Selection of conserved blocks from multiple alignments for their use in phylogenetic analysis. Mol. Biol. Evol. 17, 540–552.
- Cosson, J.F., Hutterer, R., Libois, R., Sara, M., Taberlet, P., Vogel, P., 2005. Phylogeographical footprints of the strait of Gibraltar and quaternary climatic fluctuations in the western Mediterranean: a case study with the greater white-toothed shrew, *Crocodyrus russula* (Mammalia: Soricidae). Mol. Ecol. 14, 1151–1162.
- Crochet, P.A., Dubois, A., 2004. Recent changes in the taxonomy of European amphibians and reptiles. In: Gasc, J.P., Cabela, A., Crnobrnja-Isailović, J., Dolmen, D., Grossenbacher, K., Haffner, P., Lescure, J., Martens, H., Martínez Rica, J.P., Maurin, H., Oliveira, M.E., Sofianidou, T.S., Veith, M., Zuidervijk, A. (Eds.), Atlas of Amphibians and Reptiles in Europe. Re-edition. Societas Europaea Herpetologica and Muséum national d'Histoire naturelle, Paris, pp. 495–516.
- Crottini, A., Andreone, F., Kosuch, J., Borkin, L.J., Litvinchuk, S.N., Eggert, C., Veith, M., 2007. Fossorial but widespread: the phylogeography of the common spadefoot toad (*Pelobates fuscus*), and the role of the Po Valley as a major source of genetic variability. Mol. Ecol. 16, 2734–2754.
- Ding, Z.L., Xiong, S.F., Sun, J.M., Yang, S.L., Gu, Z.Y., Liu, T.S., 1999. Pedostratigraphy and paleomagnetism of a 7.0 Ma eolian loess-red clay sequence at Lingtai, Loess Plateau, north-central China and the implications for paleomonsoon evolution. Palaeogeogr. Palaeoclimat. Palaeoecol. 152, 49–66.
- Donghuai, S., Zhisheng, A., Shaw, J., Zhisheng, A., Bloemendal, J., Youbin, S., 1998. Magnetostratigraphy and palaeoclimatic significance of Late Tertiary aeolian sequences in the Chinese Loess Plateau. Geophys. J. Int. 134, 207–212.
- Drummond, A., Rambaut, A., 2007. BEAST: Bayesian evolutionary analysis by sampling trees. BMC Evol. Biol. 7, 214.
- Duellman, W.E., Trueb, L., 1994. Biology of Amphibians. John Hopkins University Press, Baltimore, MD.
- Fauquette, S., Suc, J.P., Bertini, A., Popescu, S.M., Warny, S., Taoufiq, N.B., Villa, M.J.P., Chikhi, H., Feddi, N., Subally, D., Clauzon, G., Ferrier, J., 2006. How much did climate force the Messinian salinity crisis? Quantified climatic conditions from pollen records in the Mediterranean region. Palaeogeogr. Palaeoclimat. Palaeoecol. 238, 281–301.
- Felsenstein, J., 1985. Confidence limits on phylogenies: An approach using the bootstrap. Evolution 39, 783–791.
- Fortelius, M., Eronen, J., Jernvall, J., Liu, L., Pushkina, D., Rinne, J., Tesakov, A., Vislobokova, I., Zhang, Z., Zhou, L., 2002. Fossil mammals resolve regional patterns of Eurasian climate change over 20 million years. Evol. Ecol. Res. 4, 1005–1016.
- Fortelius, M., Eronen, J., Liu, L., Pushkina, D., Tesakov, A., Vislobokova, I., Zhang, Z., 2006. Late Miocene and Pliocene large land mammals and climatic changes in Eurasia. Palaeogeogr. Palaeoclimat. Palaeoecol. 238, 219–227.
- Fromhage, L., Vences, M., Veith, M., 2004. Testing alternative vicariance scenarios in Western Mediterranean discoglossid frogs. Mol. Phylogenet. Evol. 31, 308–332.
- Frost, D.R., 2011. Amphibian Species of the World: an Online Reference. Version 5.5. <<http://research.amnh.org/vz/herpetology/amphibia/>> (31.01.11).
- Gasc, J.P., Cabela, A., Crnobrnja-Isailović, J., Dolmen, D., Grossenbacher, K., Haffner, P., Lescure, J., Martens, H., Martínez Rica, J.P., Maurin, H., Oliveira, M.E., Sofianidou, T.S., Veith, M., Zuidervijk, A. (Eds.), 1997. Atlas of amphibians and reptiles in Europe. Collection Patrimoines Naturels, 29, Societas Europaea Herpetologica, Muséum National d'Histoire naturelle & Service du Patrimoine Naturel, Paris.
- Geniez, P., Cheylan, M., 2005. Reptiles et Batraciens de France. CD-rom, Educagri, Dijon.
- Geniez, P., Cheylan, M., in press. Les Amphibiens et les Reptiles du Languedoc-Roussillon et régions limitrophes. Atlas biogéographique. Meridionalis, EPHE & Biotope, Mèze (France).
- Gómez, A., Lunt, D., 2007. Refugia within Refugia: patterns of Phylogeographic Concordance in the Iberian Peninsula. In: Weis, N., Ferrand, N. (Eds.), Phylogeography of Southern European Refugia. Springer, pp. 155–188.
- Grassi, F., De Mattia, F., Zecca, G., Sala, F., Labra, M., 2008. Historical isolation and quaternary range expansion of divergent lineages in wild grapevine. Biol. J. Linnean Soc. 95, 611–619.
- Grill, A., Amori, G., Aloise, G., Lisi, I., Tosi, G., Wauters, L.A., Randi, E., 2009. Molecular phylogeography of European *Sciurus vulgaris*: refuge within refugia? Mol. Ecol. 18, 2687–2699.
- Guicking, D., Lawson, R., Joger, U., Wink, M., 2006. Evolution and phylogeny of the genus *Natrix* (Serpentes: Colubridae). Biol. J. Linnean Soc. 87, 127–143.
- Guo, Z.T., Sun, B., Zhang, Z.S., Peng, S.Z., Xiao, G.Q., Ge, J.Y., Hao, Q.Z., Qiao, Y.S., Liang, M.Y., Liu, J.F., Yin, Q.Z., Wei, J.J., 2008. A major reorganization of Asian climate by the early Miocene. Climate Past 4, 153–174.
- Harris, D.J., Batista, V., Carretero, M.A., 2003. Diversity of 12S mitochondrial DNA sequences in Iberian and northwest African water frogs across predicted geographic barriers. Herpetozoa 16, 81–83.
- Hewitt, G., 2000. The genetic legacy of the quaternary ice ages. Nature 405, 907–913.
- Hijmans, R.J., Cameron, S.E., Parra, J.L., Jones, P.G., Jarvis, A., 2005. Very high resolution interpolated climate surfaces for global land areas. Int. J. Climatol. 25, 1965–1978.
- Ho, S.Y.W., Saarma, U., Barnett, R., Haile, J., Shapiro, B., 2008. The effect of inappropriate calibration: three case studies in molecular ecology. PLoS ONE 3, 1–8.
- Horn, A., Roux-Morabito, G., Lieutier, F., Kerdelhué, C., 2006. Phylogeographic structure and past history of the circum-Mediterranean species *Tomicus destruens* Woll. (Coleoptera: Scolytinae). Mol. Ecol. 15, 1603–1615.
- Igawa, T., Kurabayashi, A., Nishioka, M., Sumida, M., 2006. Molecular phylogenetic relationship of toads distributed in the Far East and Europe inferred from the nucleotide sequences of mitochondrial DNA genes. Mol. Phylogenet. Evol. 38, 250–260.
- Joger, U., Fritz, U., Guicking, D., Kalyabina-Hauf, S., Nagy, T.T., Wink, M., 2010. Relict populations and endemic clades in Palaeartic refugia: evolutionary history and implications for conservation. In: Hebel, J.C., Assmann, T. (Eds.), Relict Species: Phylogeography and Conservation Biology. Springer, pp. 119–143.
- Jost, A., Fauquette, S., Kageyama, M., Krinner, G., Ramstein, G., Suc, J.-P., Violette, S., 2009. High resolution climate and vegetation simulations of the Late Pliocene, a model-data comparison over western Europe and the Mediterranean region. Climate Past 5, 585–606.
- Katoh, K., Misawa, K., Kuma, K., Miyata, T., 2002. MAFFT: a novel method for rapid multiple sequence alignment based on fast Fourier transform. Nucl. Acids Res. 30, 3059–3066.
- Klicka, J., Zink, R.M., 1997. The importance of recent ice ages in speciation: a failed paradigm. Science 277, 1666–1669.

- Kozak, K.H., Graham, C.H., Wiens, J.J., 2008. Integrating GIS-based environmental data into evolutionary biology. *Trends Ecol. Evol.* 23, 141–148.
- Kuttrup, B., Yilmaz, N., Canakci, S., Belduz, A.O., Doglio, S., 2006. Intraspecific variation of *Bufo bufo*, based on 16S ribosomal RNA sequences. *Amphibia-Reptilia* 27, 268–273.
- Litvinchuk, S.N., Borkin, L.J., Skorinov, D.V., Rosanov, J.M., 2008. A new species of common toads from the Talysch Mountains, south-eastern Caucasus: genome size, allozyme, and morphological evidences. *Russ. J. Herpetol.* 15, 19–43.
- Liu, L., Eronen, J.T., Fortelius, M., 2009. Significant mid-latitude aridity in the middle Miocene of East Asia. *Palaeogeogr. Palaeoclimat. Palaeoecol.* 279, 201–206.
- Lizana, M., 2002. *Bufo bufo* (Linnaeus, 1758). Sapo común, escuerzo. In: Pleguezuelos, J.M., Marquez, R., Lizana, M. (Eds.), *Atlas y libro rojo de los anfibios y reptiles de España. De Medio Ambiente, Madrid*, pp. 103–108.
- Llorente, G.A., Montori, A., Santos, X., Carretero, M.A., 1995. *Atlas dels amfibis i rèptils de Catalunya i Andorra*. Ed. El Brau, Barcelona.
- Ma, Y.Z., Li, J.J., Fang, X.M., 1998. Pollen assemblage in 30.6–5.0 Ma redbeds of Linxia region and climate evolution. *Chin. Sci. Bull.* 43, 301–304.
- Maddison, W.P., Maddison, D.R., 2009. Mesquite: A Modular System for Evolutionary Analysis. Version 2.72. <<http://mesquiteproject.org>>.
- Marshall, D.C., 2010. Cryptic failure of partitioned Bayesian phylogenetic analyses: lost in the land of long trees. *Syst. Biol.* 59, 108–117.
- Martinez-Solano, I., Gonzalez, E.G., 2008. Patterns of gene flow and source-sink dynamics in high altitude populations of the common toad *Bufo bufo* (Anura: Bufonidae). *Biol. J. Linnean Soc.* 95, 824–839.
- Mattoccia, M., Romano, A., Sbordoni, V., 2005. Mitochondrial DNA sequence analysis of the spectacled salamander, *Salamandrina terdigitata* (Urodela: Salamandridae), supports the existence of two distinct species. *Zootaxa* 995, 1–19.
- Measey, G.J., Vences, M., Drewes, R.C., Chiari, Y., Melo, M., Bourles, M., 2007. Freshwater paths across the ocean: molecular phylogeny of the frog *Ptychocheilus newtoni* gives insights into amphibian colonization of oceanic islands. *J. Biogeogr.* 34, 7–20.
- Mein, P., 1999. European Miocene mammal biochronology. In: Rössner, G.E., Heissig, K. (Eds.), *The Miocene Land Mammals of Europe*. Verlag Dr. Friedrich Pfeil, Munich, pp. 25–38.
- Melville, J., Hale, J., Mantziou, G., Ananjeva, N.B., Milto, K., Clemann, N., 2009. Historical biogeography, phylogenetic relationships and intraspecific diversity of agamid lizards in the Central Asian deserts of Kazakhstan and Uzbekistan. *Mol. Phylogenet. Evol.* 53, 99–112.
- Mertens, R., Wermuth, H., 1960. *Die Amphibien und Reptilien Europas*. W. Kramer, Frankfurt am Main.
- Molnar, P., Boos, W.R., Battisti, D.S., 2010. Orographic controls on climate and paleoclimate in Asia: thermal and mechanical roles for the Tibetan Plateau. *Ann. Rev. Earth Planet. Sci.* 38, 77–102.
- Muratet, J., 2008. *Identifier les Amphibiens de France métropolitaine*. Association Ecodiv. Collection, Guide de terrain.
- Nascetti, G., Zangari, F., Canestrelli, D., 2005. The spectacled salamanders, *Salamandrina terdigitata* (Lacépède, 1788) and *S. perspicillata* (Savi, 1821): genetic differentiation and evolutionary history. *Rend. Fis. Acc. Lincei* 16, 159–169.
- Nei, M., 1978. Estimation of average heterozygosity and genetic distance from a small number of individuals. *Proc. Natl. Acad. Sci.* 70, 3321–3323.
- Nogués-Bravo, D., 2009. Predicting the past distribution of species climatic niches. *Glob. Ecol. Biogeogr.* 18, 521–531.
- Palo, J.U., Schmeller, D.S., Laurila, A., Primmer, C.R., Kuzmin, S.L., Merilä, J., 2004. High degree of population subdivision in a widespread amphibian. *Mol. Ecol.* 13, 2631–2644.
- Paulo, O.S., Dias, C., Bruford, M.W., Jordan, W.C., Nichols, R.A., 2001. The persistence of Pliocene populations through the Pleistocene climatic cycles: evidence from the phylogeography of an Iberian lizard. *Proc. Roy. Soc. London B* 268, 1625–1630.
- Paulo, O.S., Pinheiro, J., Miraldo, A., Bruford, M.W., Jordan, W.C., Nichols, R.A., 2008. The role of vicariance vs dispersal in shaping genetic patterns in ocellated lizard species in the Western Mediterranean. *Mol. Ecol.* 17, 1535–1551.
- Phillips, S.J., Dudík, M., 2008. Modeling of species distributions with Maxent: new extensions and a comprehensive evaluation. *Ecography* 31, 161–175.
- Phillips, S.J., Anderson, R.P., Schapire, R.E., 2006. Maximum entropy modeling of species geographic distributions. *Ecol. Model.* 190, 231–259.
- Pleguezuelos, J.M., Fahd, S., Carranza, S., 2008. El papel del Estrecho en la conformación de la actual fauna de anfibios y reptiles del Mediterráneo Occidental. *Bol. Asoc. Herpetol. Españ.* 19, 2–17.
- Popov, S.V., Shcherba, I.G., Ilyina, L.B., Nevekskaya, L.A., Paramonova, N.P., Khondkarian, S.O., Magyar, I., 2006. Late Miocene to Pliocene palaeogeography of the Paratethys and its relation to the Mediterranean. *Palaeogeogr. Palaeoclimat. Palaeoecol.* 238, 91–106.
- Posada, D., 2008. JModelTest: phylogenetic model averaging. *Mol. Biol. Evol.* 25, 1253–1256.
- Prumuk, J.B., Robertson, T., Sites, J.W., Noonan, B.P., 2007. Around the world in 10 million years: biogeography of the nearly cosmopolitan true toads (Anura: Bufonidae). *Glob. Ecol. Biogeogr.* 17, 72–83.
- Qiang, X., Li, Z., Powell, C., Zheng, H., 2001. Magnetostratigraphic record of the Late Miocene onset of the East Asian monsoon, and Pliocene uplift of northern Tibet. *Earth Planet. Sci. Lett.* 187, 83–93.
- Rage, J.-C., Roček, Z., 2003. Evolution of anuran assemblages in the Tertiary and Quaternary of Europe, in the context of palaeoclimate and palaeogeography. *Amphibia-Reptilia* 24, 133–167.
- Rambaut, A., Drummond, A.J., 2007. Tracer v1.4. <<http://beast.bio.ed.ac.uk/Tracer>>.
- Randi, E., 2007. Phylogeography of South European mammals. In: Weiss, S., Ferrand, N. (Eds.), *Phylogeography of Southern European Refugia*. Springer, pp. 101–126.
- Recuero, E., Iraola, A., Rubio, X., Machordom, A., Garcia-Paris, M., 2007. Mitochondrial differentiation and biogeography of *Hyla meridionalis* (Anura: Hylidae): an unusual phylogeographical pattern. *J. Biogeogr.* 34, 1207–1219.
- Roelants, K., Bossuyt, F., 2005. Archaeobatrachian paraphyly and Pangaeian diversification of crown-group frogs. *Syst. Biol.* 54, 111–126.
- Roelants, K., Gower, D.J., Wilkinson, M., Loader, S.P., Biju, S.D., Guillaume, K., Moriau, L., Bossuyt, F., 2007. Global patterns of diversification in the history of modern amphibians. *PNAS* 104, 887–892.
- Ronquist, F., Huelsenbeck, J.P., 2003. MrBayes 3: Bayesian phylogenetic inference under mixed models. *Bioinformatics* 19, 1572–1574.
- Rowe, G., Harris, D.J., Beebe, T.J., 2006. Lusitania revisited: a phylogeographic analysis of the natterjack toad *Bufo calamita* across its entire biogeographical range. *Mol. Phylogenet. Evol.* 39, 335–346.
- Saitou, N., Nei, M., 1987. The neighbor-joining method: a new method for reconstructing of phylogenetic trees. *Mol. Biol. Evol.* 4, 406–425.
- Santucci, F., Nascetti, G., 1996. Hybrid zones between two genetically differentiated forms of the pond frog *Rana lessonae* in southern Italy. *J. Evol. Biol.* 9, 429–450.
- Savage, J.M., 1973. The geographic distributions of frogs: patterns and predictions. In: Vial, J.L. (Ed.), *Evolutionary Biology of Anurans*. University of Missouri Press, Columbia, pp. 351–445.
- Schmitt, T., 2007. Molecular biogeography of Europe: Pleistocene cycles and postglacial trends. *Front. Zool.* 4, 11.
- Seddou, J.M., Santucci, F., Reeve, N.J., Hewitt, G.M., 2001. DNA footprints of European hedgehogs, *Erinaceus europaeus* and *E. concolor*: Pleistocene refugia, postglacial expansion and colonization routes. *Mol. Ecol.* 10, 2187–2198.
- Seppä, P., Laurila, A., 1999. Genetic structure of island populations of the anurans *Rana temporaria* and *Bufo bufo*. *Hereditas* 82, 309–317.
- Sexton, J.P., McIntyre, P.J., Angert, A.L., Rice, K.J., 2009. Evolution and ecology of species range limits. *Ann. Rev. Ecol. Syst.* 40, 415–436.
- Shimodaira, H., 2002. An approximately unbiased test of phylogenetic tree selection. *Syst. Biol.* 51, 492.
- Shimodaira, H., Hasegawa, M., 2001. CONSEL: for assessing the confidence of phylogenetic tree selection. *Bioinformatics* 17, 1246–1247.
- Soloumian, N., Plavcan, J.M., Quade, J., Witmer, L., 1999. The paleoecology of the Pikermian Biome and the sacanna myth. In: Agustí, J., Rook, L., Andrews, P. (Eds.), *Evolution of Neogene Terrestrial Ecosystems in Europe*. Cambridge University Press, pp. 436–453.
- Soria-Carrasco, V., Castresana, J., 2011. Patterns of mammalian diversification in recent evolutionary times: global tendencies and methodological issues. *J. Evol. Biol.* 24, 2611–2623.
- Stamatakis, A., 2006. RAxML-VI-HPC: maximum likelihood-based phylogenetic analyses with thousands of taxa and mixed models. *Bioinformatics* 22, 2688–2690.
- Stewart, J., Lister, A., 2001. Cryptic northern refugia and the origins of the modern biota. *Trends Ecol. Evol.* 16, 608–613.
- Stöck, M., Dubey, S., Klütsch, C., Litvinchuk, S.N., Scheidt, U., Perrin, N., 2008a. Mitochondrial and nuclear phylogeny of circum-Mediterranean tree frogs from the *Hyla arborea* group. *Mol. Phylogenet. Evol.* 49, 19–102.
- Stöck, M., Sicilia, A., Belfiore, N.M., Buckley, D., Lo Brutto, S., Lo Valvo, M., Arculeo, M., 2008b. Post-Messinian evolutionary relationships across the Sicilian channel: mitochondrial and nuclear markers link a new green toad from Sicily to African relatives. *BMC Evol. Biol.* 8, 56.
- Sun, J., Ye, J., Wu, W., Ye, J., Wu, W., Ni, X., Bi, S., Zhang, Z., Liu, Z., Meng, J., 2010. Late oligocene-miocene mid-latitude aridification and wind patterns in the Asian interior. *Geology* 38, 515–518.
- Sun, X., Wang, P., 2005. How old is the Asian monsoon system? Palaeobotanical records from China. *Palaeogeogr. Palaeoclimat. Palaeoecol.* 222, 181–222.
- Svenning, J., Normand, S., Kageyama, M., 2008. Glacial refugia of temperate trees in Europe: insights from species distribution modeling. *J. Ecol.* 96, 1117–1127.
- Swofford, D.L., Selander, R.B., 1981. BIOSYS-1. A Computer Program for the Analysis of Allelic Variation in Population Genetics and Biochemical Systematics. Illinois Nat. Hist. Survey, Champaign.
- Tamura, K., Peterson, D., Peterson, N., Stecher, G., Nei, M., Kumar, S., 2011. MEGA5: molecular evolutionary genetics analysis using maximum likelihood, evolutionary distance, and maximum parsimony methods. *Mol. Biol. Evol.* 28, 2731–2739.
- Tarasov, P.E., Volkova, V.S., Webb III, T., Guiot, J., Andreev, A.A., Bezusko, L.G., Bezusko, T.V., Bykova, G.V., Dorofeyuk, N.I., Kvavadze, E.V., Osipova, I.M., Panova, N.K., Sevastyanov, D.V., 2000. Last glacial maximum biomes reconstructed from pollen and plant macrofossil data from northern Eurasia. *J. Biogeogr.* 27, 609–620.
- Ursenbacher, S., Schweiger, S., Tomovic, L., Crnobrnja-Isailović, J., Fumagalli, L., Mayer, W., 2008. Molecular phylogeography of the nose-horned viper (*Vipera ammodytes* Linnaeus, 1758): evidence for high genetic diversity and multiple refugia in the Balkan Peninsula. *Mol. Phylogenet. Evol.* 46, 1116–1128.
- Van Bocxlaer, I., Biju, S., Loader, S., Bossuyt, F., 2009. Toad radiation reveals into-India dispersal as a source of endemism in the Western Ghats-Sri Lanka biodiversity hotspot. *BMC Evol. Biol.* 9, 131.
- Van Bocxlaer, I., Loader, S.P., Roelants, K., Biju, S.D., Menegon, M., Bossuyt, F., 2010. Gradual adaptation toward a range-expansion phenotype initiated the global radiation of toads. *Science* 327, 679–682.
- Van Dam, J.A., 2006. Geographic and temporal patterns in the late Neogene (12–3 Ma) aridification of Europe: the use of small mammals as paleoprecipitation proxies. *Palaeogeogr. Palaeoclimat. Palaeoecol.* 238, 190–218.

- Veith, M., Mayer, C., Samraoui, B., Donaire Barroso, D., Bogaerts, S., 2004. From Europe to Africa and *viceversa*: evidence for multiple intercontinental dispersal in ribbed salamanders (Genus *Pleurodeles*). *J. Biogeogr.* 31, 159–171.
- Vences, M., Vieites, D.R., Glaw, F., Brinkmann, H., Kosuch, J., Veith, M., Meyer, A., 2003. Multiple overseas dispersal in amphibians. *Proc. Roy. Soc. London B* 270, 2435–2442.
- Voelker, G., 1999. Dispersal, vicariance, and clocks: historical biogeography and speciation in a cosmopolitan passerine genus (*Anthus*: Motacillidae). *Evolution* 53, 1536–1552.
- Waltari, E., Hijmans, R.J., Peterson, A.T., Nyári, Á.S., Perkins, S.L., Guralnick, R.P., 2007. Locating pleistocene refugia: comparing phylogeographic and ecological niche model predictions. *PLoS ONE* 2, e563.
- Wan, S., Li, A., Clift, P.D., 2007. Development of the East Asian monsoon: mineralogical and Sedimentologic records in the northern South China Sea since 20 Ma. *Palaeogeogr. Palaeoclimat. Palaeoecol.* 254, 561–582.
- Wiens, J.J., 2000. Reconstructing phylogenies from allozyme data: comparing method performance with congruence. *Biol. J. Linn. Soc.* 70, 613–632.
- Williams, S.E., Bolitho, E.E., Fox, S., 2003. Climate change in Australian tropical rainforests: an impending environmental catastrophe. *Proc. Roy. Soc. Lond. B. Biol.* 270, 1887–1892.
- Zajc, I., Arntzen, J.W., 1999. Phylogenetic relationships of the European newts (genus *Triturus*) tested with mitochondrial DNA sequence data. *Contr. Zool.* 68, 73–81.
- Zangari, F., Cimmaruta, R., Nascetti, G., 2006. Genetic relationships of the western Mediterranean painted frogs based on allozymes and mitochondrial markers: evolutionary and taxonomic inferences (Amphibia, Anura, Discoglossidae). *Biol. J. Linnean Soc.* 87, 515–536.
- Zeisset, I., Beebee, T.J.C., 2008. Amphibian phylogeography: a model for understanding historical aspects of species distributions. *Heredity* 101, 109–119.
- Zhan, A., Fu, J., 2011. Past and present: phylogeography of the *Bufo gargarizans* species complex inferred from multi-loci allele sequence and frequency data. *Mol. Phylogenet. Evol.* 61, 136–148.
- Zheng, Y., Fu, J., Li, S., 2009. Toward understanding the distribution of Laurasian frogs: a test of Savage's biogeographical hypothesis using the genus *Bombina*. *Mol. Phylogenet. Evol.* 52, 70–83.